Research on Engineering Structures & Materials
www.jresm.org
Research Group

Research Article

Structural application of fiber reinforced concrete

Kalapala Vijay Babu*[,1,a], CH. Mallika Chowdary[1,b], Lingeshwaran N[1,c], Ikkurthi Siva Kishore[2,d]

[1]*Dept. of Civil Eng., Koneru Lakshmaiah Education Foundation (Deemed to be University), Guntur, India*
[2]*Dept. of Civil, Construction and Environmental Engineering, Iowa State University, Ames, IA, US*

Article Info

Article history:

Received 31 May 2024
Accepted 02 Dec 2024

Keywords:

Coir fiber;
Plastic fiber;
Stress- strain behavior;
Durability properties;
Flexural behavior;
Micro structural analysis

Abstract

This study investigates the structural application of fiber-reinforced concrete using coir and plastic fibers. The experiment incorporated various percentages of fibers in concrete: coir fiber and plastic fibers at 0.5%, 1%, 1.5%, and 2%. An over-all of 80 concrete cubes, 42 cylinders, and 40 prisms were cast and examined to assess various mechanical properties. Compressive strength, and durability tests were conducted on the concrete cubes. The cylinders were subjected to split tensile tests and stress-strain behavior evaluations. The prisms underwent flexural strength tests to determine their performance under load. Additionally, the study included reinforced concrete beams reinforced with steel and fibers, and one beam with fibers only. Flexural strength tests were conducted on these beams, resulting in stress-strain behavior and load-deflection. Advanced characterization techniques such as Scanning Electron Microscopy (SEM), Energy Dispersive X-ray (EDX), and Fourier Transform Infrared Spectroscopy (FTIR) were applied to end sample powders of both normal and optimized mixes The findings indicate that the incorporation of 1% coir and plastic fibers significantly enhances the mechanical performance of concrete. The results from compressive strength, tensile strength, and flexural strength tests recommend that fiber reinforcement improves the durability and structural integrity of concrete. The SEM, EDX, and FTIR analyses provided insights into the microstructural changes and bonding characteristics of the fiber-reinforced concrete, corroborating the mechanical test outcomes. In conclusion, the study demonstrates that fiber-reinforced concrete, particularly with 1% coir and plastic fibers, the 1% of coir sample increased tensile strength by 10% and flexural strength by 20%, while the 1% plastic fiber improved flexural strength by 50% and split tensile strength by 30%. It is a viable and sustainable option for enhancing the mechanical performance and durability of concrete structures. This creative approach has potential for building environmentally friendly concrete infrastructure.

1.Introduction

The construction industry is heavily dependent on the extraction and use of natural resources, though, due to the materials' production and transportation to the construction site, which uses a considerable quantity of non-renewable resources and releases a substantial amount of carbon dioxide [1]. Concrete, a popular building material due to its strength, durability, and flexibility, has faced challenges in modern building processes. Low tensile and flexural strength, which increases the risk of breaking under strain, and the high CO_2 releases from concrete buildings have negative environmental impacts. Therefore, there is an increasing consumer demand for ecologically sustainable

*Corresponding author: kalapalavijay122@gmail.com
[a] orcid.org/0009-0000-4876-848X; [b] orcid.org/0000-0001-6888-0364; [c] orcid.org/0000-0003-2998-7315; [d] orcid.org/0000-0002-9143-0027
DOI: http://dx.doi.org/10.17515/resm2024.305st0531rs

construction materials with higher quality. Research is being conducted to explore alternative materials like industrial, home, and recyclable resources, which can support environmental harmony and contribute to sustainable development goals [2][3][4]. Aggregate, bound by slurry and water, forms a solid mass. It's an adaptable construction material, used for various purposes. Engineers can use additives and admixtures to modify concrete properties [5]. Certain loading stages influence how cementitious composites that include two or more blended fibers respond to the cracking process. The finished product that incorporates two or more fibers is referred to as "fiber reinforced concrete. Fibers perform better than the sum of their parts when combined, which is why fiber-reinforced concretes are constructed with a range of fiber types integrated [6].

FRC behaviour is influenced by fiber type, shape, orientation, aspect ratio, and content. Steel and basalt fibers are added to Ultra-High-Performance Concrete (UHPC) to improve tensile strength, hydration, and low pre-crack energy absorption [7]. CFRP composites offer numerous benefits over traditional materials, including durability, high strength, lightweight, and quick installation, making them increasingly used in the construction industry for infrastructure applications [8].

A brittle behaviour characterizes plain concrete in tension because of the low tensile strength, and the reduced strain capacity. The addition of randomly distributed fibers to plane concrete has been shown to provide higher ductility and strength. The fibers transfer stresses between the concrete matrix and tensile strains during the crack propagation, thus improving the post-cracking response. The main parameters affecting the design and performance of FRC are the fiber volume content (V_f), the ratio between the length and the diameter of fibers (l/d), and the fiber weight ratio (FWR), defined as the weight of the fibers in 1 m^3. In particular, the l/d ratio affects the number of fibers which cross the cracks under load, keeping constant V_f. Because of the importance of the fiber dimensions, the industry makes available different types and sizes of this reinforcement, ranging from 6 mm to a maximum length of 80 mm and from 0.1 to a maximum cross section area of 1.5 mm^2 [9].

C. Lin et.al[10]-classified features that include the reinforcement as well as the fibers as variables impacting the bonding among the fibers and the concrete matrix. Bonding strength may be increased by improving the concrete matrix's strength, which is directly related to how compact it is. By directly altering binder powder particle packing and wall effect, multiscale reinforcement of the environment with ingredients such as fly ash, silica fume, nanotubes, and micro or nanofillers can improve bonding characteristics and strengthen the fiber-matrix interface. Depending on the matrix and fiber characteristics, the ITZ's width can range from nanometers to micrometers. The surface area of the fiber is typically greater than its geometrical value because of these holes and microcracks. The efficiency of the method at the fiber-matrix interface is further examined using a variation of other micro-characterization methods, with scanning electron microscopy (SEM), Fourier transform infrared (FTIR) spectroscopy, nano-indentation, etc.

Jamal A. Abdalla et. al. [11] classify the constitutive behaviour of fiber reinforced composites at various strain rates as being shown to be greatly affected by the natural filler qualities, amounts, sizes, and kinds of matrix polymers.K. Sandeep Dutt et. al [12] Shows that Performance under varied strain rates can be enhanced by increasing the fiber-matrix stress-transfer efficiency by optimizing these variables. Composites reinforced with flax and jute fibres were found to be stiffer than those reinforced with cotton fibres, despite the fact that all materials have a potential to grow more rigid with rising strain rates.

The high concentration of natural fibers in many developing nations, together with additional relevant elements, demands that scientists and engineers use the right technology to maximize use of these fibers for structural upgrades and, additionally, other uses like housing and other requirements. There are plenty of natural resources available

to us, and we must continue to explore them. The emergence of plant fiber composites is quite new. Numerous different natural fibers, primarily produced in India, including jute, coir, banana, and sisal, are among the fiber-reinforced composites that are of special interest because they have moderate tensile and flexural properties in addition to strong impact resistance in comparison to other plant-based fibers [13, 15].

A. N. Kangu et.al [16] & U. Sharma et.al [17] added fibers to the concrete in specific portions, to improve its performance. The structural stability of concrete is increased by adding fibers. The fibers were cut into 40mm lengths and additional to the concrete at concentrations of 0.5%, 1%, 1.5%, and 2%. The mechanical properties, such as Tension, Flexure, and Compression strengths were examined to indicate the contribution of the fibers in concrete. The findings indicate prevention of cracks on adding fibers, thereby the stress-bearing capacity of concrete can be enhanced. Natural fiber-containing concrete mixes are ideal for civil construction, tunnelling, industrial floors, and foundation slabs. However, studies on high-strength concrete have not thoroughly examined the combined impacts of supplementary cementitious materials and natural fiber concentrations. These large, low-cost, and easy-to-manufactured composites are increasingly used in industries like paper fabrication, automobiles, and aircraft furniture due to their ecological benefits [18].

Bamboo leaf ash (BLA) is a renewable resource with pozzolanic reactivity, but its improper use leads to environmental harm. A sustainable solution is to activate Bamboo leaf ash (BLA) pozzolanic reactivity through controlled calcination. A study explores blending Portland-limestone cement and Bamboo leaf ash (BLA) in high performance concrete manufacturing to raise awareness among building industry experts about alternative materials in construction projects [19]. Fiber Reinforced Polymer (FRP) sheets are used, especially for seismic retrofitting, to boost the flexural capacity of reinforced concrete beams and columns. For FRP sheets, synthetic fibers are often utilized. However, because of their high cost and environmental problems arising from recycling issues, natural fibers are utilized to generate Natural Fiber Reinforced Polymer, or NFRP. NFRP provides a synthetic fiber substitute that is less harmful to the environment. The analysis of the bond strength between natural fiber reinforced polymer (NFRP) sheets and concrete [20,22].

The utilization of natural fibers resulting from plants such as jute, hemp, sisal, sugar cane, cannabis, bamboo, coconut, and banana are recommended for concrete because of their low cost, availability, and easy of handling. Coconut fiber is a biodegradable and renewable resource that might be used to strengthen concrete. This can improve the material's mechanical qualities, such as tensile strength and flexibility, and increase its resistance to damage and cracking [23]. The compressive strength of concrete with waste PET fibers is influenced by particle shape, concentration, and water cement ratio. Up to 1.0% of PET fibers can improve concrete performance due to their consistent fibrous structure. However, adding more than 1.0% was a reduction in the compressive strength of concrete, which is likely connected to PET surfaces' poor reactivity, low absorption qualities, reduced hydration, instability, and low friction coefficient. Waste polyethylene terephthalate (PET) can be used as recycled resin by depolymerizing it with nanocatalysts, reducing porosity and increasing durability. This study examined the flexural behavior of glass fiber reinforced polymer Reinforced polymer (GFRP RC) beams and concrete incorporating PET waste fiber. The results provide fresh directions for investigation into flexure structural elements. The study examined the effect of adding PET fiber to concrete on cracking behavior, ultimate load capacity, and mode of failure. Flexural analysis was shown for beams reinforced with PET bar to calculate strain and understand load-deflection response [24, 27].

Concrete's tensile strength has been improved by the use of various fibers over the past decade, including natural, synthetic, metallic, and mineral fibers. Steel fibers are the most commonly used due to their excellent mechanical properties. The distribution of fibers in concrete is crucial for uniform reinforcing, as they can have various geometric characteristics. Steel fibers prevent crack formation and improve ductility, increasing tensile strength and post-crack reaction, making concrete more ductile and stronger under varied loads [28, 29]. This study explores the use of fibers like steel and glass fiber to improve the flexural strength and ductility of printed beams. These fibers are increasingly popular due to their financial and mechanical benefits. Glass fibers enhance mechanical properties, while steel fibers have been shown to affect the flexural strength and ductility of concrete components [30][31].

The study explores the relationship between fiber length and Ultra-high-performance fiber-reinforced concrete (UHPFRC's) tensile characteristics, finding that the type of fiber affects porosity and tensile strength distribution. The seismic performance of bridge piers is made of UHPFRC, using the modified Kent-Park model to describe the compressive stress-strain relationship of UHPFRC. The study emphasizes the importance of numerical simulation in designing UHPC/UHPFRC structures and suggests combining probabilistic analysis with UHPC fracture modelling for further investigation [32]. Salah Al-Jasmi et. al. research study on utilizes the ANSYS software and finite element analysis to design reinforced concrete beams for off-site oil and gas plants. The simulation environment aids in blast-resistant concrete structure design by generating beam models. The research fills gaps in engineering literature on blast-resistant concrete beam design, thereby enhancing scientific understanding and filling gaps in engineering literature [33][34]. Ultra-high-performance concrete (UHPC) uses steel fibers to withstand less tensile load at crack surfaces, enhancing the moment capacity of reinforced beams. The strong bond between rebar and UHPFRC reduces development length by 20-30% compared to ordinary concrete [35].

Layla K. Amaireh et. al. [36] classify the flexural strength of reinforced concrete beams has been enhanced by a number of methods, such as externally bonded steel plates, FRP strips, RC jacketing, and steel fiber reinforced concrete (SFRC). These techniques do have several drawbacks, though, including brittleness, limited fire resistance, low interfacial bond strength, and hazardous fume emission. A material with the necessary ductility and strength retention at high temperatures is required to reinforce for reinforced concrete structures. High ductility, fire resistance, and strength retention are characteristics of steel and polyvinyl-alcohol hybrid fiber-reinforced engineered cementitious composite (SPH-ECC) that indicate possibility. To look into these factors, ABAQUS finite element analysis and Experiments were conducted.

Seyed Fathollah Sajedi et. al. [37] research aims to determine the optimal arrangement and amount of CFRP composites for strengthening externally reinforced concrete beams, considering concrete strength and contact type. Various CFRP composite configurations were used, and nonlinear finite element analysis was conducted using ABAQUS to model and assess this behavior needed for reinforcing concrete structures.

Transverse rebars offer more confinement and avoid buckling, while increasing the longitudinal reinforcement ratio improves ductility in axially loaded GFRP-RC and CFRP-RC columns, according to research[38]. The numerical model's key aspects include determining the FE dimension, selecting constitutive models for steel fiber reinforced expanded-shale lightweight concrete (SFRELC), steel bars, and bond-slip behavior, defining the loading method, and establishing the convergence criterion. The FE dimension's accuracy and software efficiency depend on its size, with the smallest dimension being the size of coarse aggregate. [39].

This research fits well with many of the research gaps identified in the literature review, especially regarding fiber-matrix interaction, natural fiber performance, and comparative studies between natural and synthetic fibers. However, there are opportunities for further research in areas like long-term durability, environmental impact assessment, and performance under extreme conditions. These additional investigations could significantly enhance the value of any research in the field of fiber-reinforced concrete.

This research attempted to assess the impact of incorporating fiber materials like coir and plastic in reinforced concrete beam construction to improve their structural properties. The research focused on evaluating how fibers affect the interaction of material and prevent tensile stresses. Fibers typically enhance the tensile strength of concrete and affect the ultimate shear capacity. To compare plastic and coir fibers, hemp coir rope was prepared with a thickness of 3 mm instead of adding coir fiber directly to the concrete. The physical characteristics of the plastic fibers resemble those of the coir hemp rope, similar to a 3 mm thick plastic rope cut into 50 mm length pieces. The coir fiber was divided into 50 mm × 3 mm pieces. Natural fiber reinforcements are a combination of matrix components and natural fibers, which are widely used in various fields due to their accessibility, abundance, and ease of use. These composites are thought to be eco-friendly. due to their production from plant waste, reducing their cost and being used in various industries.

2. Experimental Work

2.1. Materials

2.1.1. Concrete

To ensure the accuracy and quality of our concrete mixes, we strictly follow set norms and procedures in our trial work. OPC 53 Grade cement conforming to IS 12269: 2013, Cement properties are exposed in Table 1. Natural river fine aggregate meeting IS 383: 2016 Zone II requirements, and coarse aggregate with 30% of 10 mm and 70% of 20 mm sizes as per IS 383: 2016 are among our products.

Table 1. Properties of cement following laboratory testing

Test Performed	Value
Fineness (Sieving by 90 mm sieve)	225 m^2/kg
Specific gravity	3.15
Standard consistency	33%
Initial setting time	45 Minutes
Final setting time	8 hours 35 Minutes

Table 2. Physical properties of aggregates

Property	Fine Aggregates	Coarse Aggregate
Density kg/m^3	1.69	1.61
Water %	2	0.47
Fineness modules	3.26	3.2
Max Dia (mm)	-	20
Zone	II	-
Specific gravity	2.65	2.92

Table 2 provides the coarse and fine aggregate's properties. In accordance with IS 456: 2000, tap water is used to ensure uniformity. Furthermore, ~~our~~ mix designs are improved

by adding HI FORZA 369 chemical admixture at 0.5% of the cementitious material, in compliance with IS 9103: 1999. ~~Our~~ The finalized mix proportions are carefully calculated through repeated experiments in accordance with the strict requirements given in IS 10262: 2016, specifically for M40 grade. This ensures optimal performance and durability in our experimental objectives.

2.1.2. Coir Fiber

The coir fiber samples were extracted through cutting, maintaining a uniform size of 50 mm in length and 3 mm in diameter, resulting in an aspect ratio of approximately 16.67≃ 17. Each fiber sample was evaluated and maintained according to the required dimensions for further analysis. It is derived from coconut husks, is a biodegradable and renewable reinforcing material that reduces the carbon footprint in concrete manufacturing. It enhances flexural, tensile strength, crack resistance, shrinkage, and creep effects. Coir fiber also improves concrete's cohesiveness and workability, accelerating construction and resulting in better surface finishes. This sustainable addition aligns with sustainability goals, promoting robust and eco-friendly built environments in the construction industry. Coir fiber shown in Fig. 1a.

2.1.3. Plastic Fiber

Synthetic polymer nylon monofilament yarn is extracted through cutting, with 50mm x 3mm with aspect ratio of 16.67≃ 17. It is a multipurpose reinforcing material used in fishing lines, textile manufacture, and construction. It is essential for improving the structural integrity and lifespan of concrete constructions because of its remarkable tensile strength, resilience, and abrasion resistance. In addition to improving performance, this novel fiber helps promote sustainable building methods by lowering the need for conventional reinforcing materials like steel, which are prone to corrosion and environmental deterioration. Plastic fiber shown in Fig. 1b.

Table 3. Mix proportions of concrete

Constituents	Proportions
Cement	415 (kg/m^3)
Water	165.3 (kg/m^3)
Fine aggregate	725.2 (kg/m^3)
Coarse aggregate	1118.5 (kg/m^3)
20mm	894.8 (kg/m^3)
10mm	223.7 (kg/m^3)
Water /cement ratio	1: 2.5

2.2. Mix Design

As per the IS:10262-2019 standard, the concrete mixture is prepared. The mix ratio is shown in the Table 3 and the concrete strength grade was M40. The finalized mix proportions are the result of several trials conducted to ensure optimal outcomes. Concrete performance by volume using two types of fibers (coir and plastic). Hi-Forza 369 is a polycarboxylate-based additive that is used as a superplasticizer. During the production process, 0.5 percent of the cementitious material by weight is added to concrete as an admixture.

(a) (b)

Fig. 1. (a) Coir fiber (b) plastic fiber

2.3. Cast Specimens

A mix design was used to construct a concrete mix for the M40 grade. The ten mixes are cast out of concrete in order to examine its performance and the impact of fiber. Fig. 2 shown the schematic model for concrete mixing. Concrete performance by volume using two types of fibers (plastic and coir), one of which is a nominal mix with 0.5% superplasticizer in the M1 (Nominal Mix). The volume percentages of fiber were 0.5%, 1%, 1.5%, and 2% added by volume of concrete. Each and every mix compressive strength will compare to the nominal and each individual mixes.

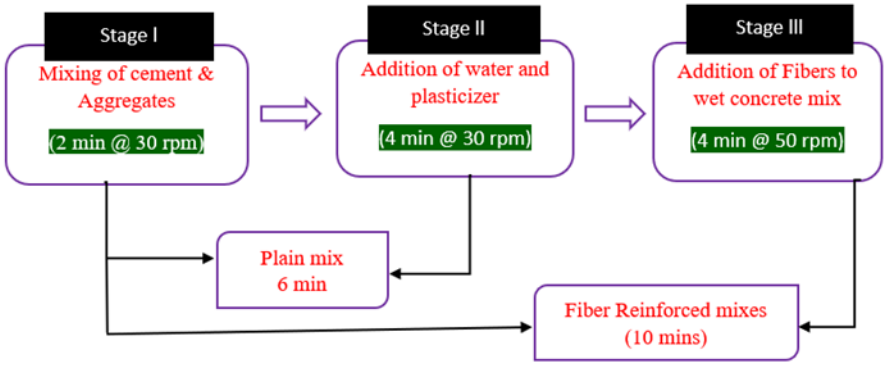

Fig. 2. Phases of mixing was carried out to generate batches of concrete [40]

The saturated, surface-dry-condition (SSD) coir fiber is used in the mixes to maintain the workability. As part of preparation, coir fiber (M1-0), (M2-0.5%C), (M3-1%C), (M4-1.5%C), (M5-2%C), and plastic fiber (M6-0.5%C), (M7-1%C), (M8-1.5%C), (M9-2%C) cast into cubes, cylinders, and prisms, etc. After 24 hours, the samples were taken out from the mould and subjected to proper curing conditions, as per standards IS 456:2000. This was done to prepare the specimens for the experimental testing. The specimens were assessed after 7, 14, 28, and 56 days of curing. Then, the split tensile, compressive, flexural, and stress strains of concrete were evaluated. On the basis of 28 days of flexural strength, split tensile strength, and compression strength, the combined mix of both the fibers, coir and plastic fibers (M10-1%CP), and 5 beams are cast to the size of 700 mm × 150 mm × 150 mm, and a nominal mix with steel reinforcement (B1-0), coir fiber (B2-1%C), plastic fiber 1% (B3-1%P), and a combined mix of both plastic and coir (B4-1%CP). B1, B2, B3, and B4

beams are cast with reinforcement and (B5-1%CP) beams without reinforcement, adding both types of fibers to the total volume of concrete.

2.4. Tests Conducted

2.4.1. Slump Test

It is a simple and widely used method to assess the workability or consistency of fresh concrete. It measures the ease with which concrete flows and is an important quality control test, especially for fiber-reinforced concrete (FRC), where the addition of fibers can affect the mix's fluidity. In the slump test, fresh concrete is placed into a conical mold (known as a slump cone) in three layers, with each layer being tamped to remove air pockets. The cone is then carefully lifted, and the vertical settlement or "slump" of the concrete is measured in millimeters.

2.5.2. Density of Concrete

This test helps in ensuring that the mix proportions are correct and that there are no significant air voids, which can reduce the strength and durability of the concrete. In the case of fiber-reinforced concrete, the inclusion of fibers may slightly alter the density, depending on the type and volume of fibers used, but it generally remains within the typical range for structural concrete. Firstly, measure the cylindrical jar (W_1). Fresh concrete is placed inside the cylinder. Until the jar is filled, compression is applied with the help of a tamping rod for at least 60 strokes for each 50mm layer. After the concrete's compression, the top surface should be level, and the fresh concrete should be weighed with the cylinder (W_2). The formula used to get the fresh concrete density $\left[\frac{[W_1 - W_2]}{[volume\ of\ the\ cylindrical\ jar]}\right] x\ 1000$.

2.5.3 Compressive Strength

2.5.3.1 Compression Strength Test for Cubes

It is one of the most important tests performed to assess the material's ability to withstand axial loads. This test measures the maximum compressive force that a concrete sample can bear before failure, giving an indication of the material's overall strength and suitability for structural applications. The compressive strength evaluation was performed on cube specimens with dimensions of 150 mm x 150 mm x 150 mm, which were tested following 7, 14, 28, and 56 days of curing. For each specified curing duration and for each concrete mix, three cubes were fabricated. Throughout the experimental procedure utilizing the compression testing apparatus, the well-prepared surface of the cube was oriented towards the upper section to facilitate the better compression process. The compression testing apparatus provides a quantifiable output reflecting the maximum load (in kN) that the concrete cube is capable of withstanding. The standard load rate for compressive strength tests of concrete according to IS 516 is 14 MPa per minute for cubes and 12 MPa per minute for cylinders.

2.5.3.2 Stress-Strain Behavior for cylinders

It describes how concrete responds to applied loads, illustrating its mechanical properties, such as elasticity, stiffness, strength, and failure mechanisms. Concrete, being a brittle material, exhibits distinct stress-strain characteristics under different loading conditions, particularly in compression, which is its primary mode of operation in structural applications. To assess the stress-strain behavior of concrete, cylindrical specimens are tested after 28 days of curing. The specimens are placed in a compression testing machine with strain gauges to measure load and deformation. A controlled load is applied until the specimen fails, while stress and strain are recorded. Initially, the behavior is elastic, followed by a nonlinear phase as microcracks form. The test continues until the concrete

reaches its peak strength and then fails. This data is used to plot the stress-strain curve. Fig. 3 shows the experimental setup for stress-strain behavior for cylinders.

Fig. 3. Setup for stress- strain behavior

2.5.4. Split Tensile Strength

It is conducted to evaluate the tensile strength of concrete, which is important since concrete is typically weak in tension. This test measures the concrete's ability to resist tension indirectly by subjecting it to compressive forces along its side, which causes tensile stresses to develop in the specimen, leading to its splitting along the vertical axis. The split tensile strength was performed on cylinder specimens with dimensions of 150 mm diameter with a length of 300mm, which was tested following 7, 14, 28, and 56 days of curing. The constant load rate for the split tensile strength of concrete, as per IS 5816:1999, is 1.2 to 2.4 MPa/min. For each specified curing duration and for each concrete mix, three cubes were cast. The cylinder is placed horizontally between the platens of a compression testing machine. Formula for calculating split tensile strength $((\pi/4)\ (d^2)\ (h))$. A compressive load(kN) is applied along the length of the cylinder at a constant rate. This load generates tensile stress across the vertical plane through the center of the cylinder, causing it to split vertically into two halves. Three specimens were tested for every mix, and the average of those results was taken.

2.5.5. Flexural Strength

It is used to determine the ability of concrete to resist bending or flexural stress. It is especially important for structural elements like beams and slabs, which are often subjected to bending in real-life applications. The test measures the tensile strength of concrete in bending and is commonly known as the modulus of rupture. Rectangular concrete beams, typically with dimensions of 150 mm × 150 mm × 500 mm, are cast and cured, usually for 28 days. The beams must be properly prepared to ensure uniformity and accurate results. The beam is placed on two supporting rollers, with a specified span length. A load is applied either at the midpoint. In a three-point test, the load is applied at the center of the beam, while in a four-point test, the load is applied at two points equidistant from the center. As the load is applied, the beam will experience tensile stress at the bottom and compressive stress at the top until it fractures. Three specimens were tested for every mix, and the average of those results was taken.

2.5.7. Water Absorption

It is used to determine the porosity of the material, which affects its durability and performance. High water absorption can lead to increased permeability, which can, in turn, lead to issues like reduced resistance to increased risk of corrosion in reinforcement. The

test measures how much water concrete absorbs over a specified period, giving an indication of the material's porosity and density. The saturation water absorption rate of concrete cubes measuring 150 mm × 150 mm × 150 mm was measured after 28 days of age of curing. The specimen initial weight is shown as W1 before to the specimen being completely submerged in water at room temperature for a certain amount of time, usually 24 hours or more. In order to eliminate any extra water that remains on the cube, the specimens are removed from the water after the submersion period and allowed to dry on the surface. Specimens are marked as W2 after surface drying.

2.5.8. Water Permeability

Concrete water permeability is crucial for its effectiveness and long-term sustainability in environments with high water exposure. The Fig. 5 shows concrete permeability setup. Factors such as compaction quality, water-to-cement ratio, pore size distribution, porosity, and curing conditions influence permeability. It is used to measures the ability of concrete to resist the penetration of water under pressure. This property is crucial for assessing the durability and longevity of concrete structures, as high permeability can lead to increased moisture ingress, which can cause issues like reinforcement corrosion and degradation of the concrete matrix. They are typically 150 mm × 150 mm × 150 mm cubes or 150 mm diameter × 300 mm cylinders. After being cured for 28 days in water at 20°C ± 2°C, the specimens are removed 24 hours before testing and stored in a controlled environment.

The test uses a permeability cell connected to a water source applying pressure between 0.5 MPa and 1 MPa. Specimens are dried at 105°C to a constant weight, cooled to room temperature, and placed in the cell. Water is then applied under pressure for 72 hours to assess permeability.

Fig. 5. Concrete permeability test setup

2.5.9. Acid Attack (H_2SO_4)

When assessing the resistance of concrete to sulfuric acid attack, a common method involves immersing 150 mm concrete cubes in a sulfuric acid solution after a standard curing period, typically 28 days. The solution used usually consists of a 4% concentration of sulfuric acid in water. This concentration is chosen to simulate realistic conditions of acid exposure that concrete structures may encounter in certain industrial or environmental settings. Over the course of the immersion period, which can extend up to 28 days, the concrete cubes are subjected to the corrosive effects of the sulfuric acid solution. They are two common forms of chemical deterioration that can significantly impact the durability and longevity of concrete structures. Acid attack occurs when

concrete is exposed to acidic environments, leading to the degradation of the concrete matrix. Acids can react with the calcium hydroxide (Ca $(OH)_2$) in the concrete, which is a key component of the cement paste, leading to its dissolution and weakening. Sulfate attack occurs when concrete is exposed to sulfate-rich environments, such as soils or groundwater with high sulfate content.

2.5.9. Sulfate Attack ($MgSO_4$)

After a 28-day curing period, 150mm cubes are submerged in a 5% magnesium sulphate solution as part of the magnesium sulphate assault on concrete. Sulfates react with the calcium aluminate phases in the cement paste, leading to the formation of expansive products that can cause cracking and deterioration. Samples cured in water for 28 days were then cured for 56 days in solutions containing 2% magnesium sulphate (MgSO4) and 5% sodium sulphate (Na2SO4). Samples are tested for a period of 90 days. Samples are weighted after being cured in MgSO4 and Na2SO4 solutions. Before conducting the compressive test, the samples are cleaned with tap water after curing and weighed. Three samples are tested for every mix, and the results are averaged.

2.5.10 Microstructural Analysis

Microstructural analysis of the fiber-reinforced concrete using coir and plastic fibers will involve examining the internal structure of the concrete at the microscopic level.

2.5.10.1 Scanning Electron Microscopy (SEM)

Scanning Electron Microscopy (SEM) was employed to examine the microstructure of fiber concrete, featuring images of the control mix and an optimized mix containing 1% each of coir and plastic fibers after twenty-eight days of curing, as depicted in Figs. 13 & 14. These SEM images illustrated the distribution, formation, and hydration products of the hydrated cement paste within the concrete. In contrast, the mix with fiber additions displayed abundant white crystals with tiny granular crystals on the surface, indicating enhanced concrete strength. The control concrete mix image of SEM revealed that the surfaces were laminated with voids and layers unhydrated products in the concrete. SEM analysis of powdered concrete end samples provides detailed insights into the material's microstructure and composition, facilitating observation of features such as aggregate distribution, porosity, hydration products, and potential defects or degradation mechanisms. This analytical process involves grinding concrete samples into a fine powder, mounting them onto SEM stubs, coating them with a conductive material, and placing them inside the SEM chamber. The focused electron beam interacts with the sample's atoms, generating signals used to produce high-resolution images revealing the morphology and composition of concrete components.

25.10.2 Energy Dispersive x- ray (EDX)

The analytical method known as energy dispersive X-ray spectroscopy, or EDS, is crucial for determining the elemental composition of several scientific fields. When used in conjunction with scanning or transmission electron microscopy (TEM or SEM), it causes a sample to be bombarded with electrons, causing it to release distinctive X-rays that are specific to each element. Identified and measured elements are present in these X-rays, which are detected by sensors. Atomic-level qualitative and quantitative material analysis is made possible by EDX, which is widely used in many different sectors.

2.5.10.3 Fourier Transform infrared Spectroscopy (FTIR)

Fourier Transform Infrared Spectroscopy (FTIR) is a strong analytical technique that is widely applied in many different domains to examine the molecular makeup of materials. Through the evaluation of a substance's absorption of infrared light at different

frequencies, Fourier transform infrared spectroscopy (FTIR) provides crucial information about the chemical bonds present in a sample. Defining the molecular structures is made easier by this absorption spectrum, which provides a thorough look at the functional groups that are present.

2.5.11. Flexural behavior of beams

Beam specimens are arranged in a simply supported condition by supporting one end by roller support and other end with hinge. Flexural test is conducted using UTM (universal Tensing Machine) with utilizing standard support conditions and standard test procedure (IS 9399: 1979). Specimens include a sample with nominal mix with steel reinforcement (B1-0), coir fiber (B2-1%C), 1% plastic fiber (B3-1%P), and a mixture of plastic and coir (B4-1%CP). In addition to these samples, a concrete beam without reinforcement (B5-1%CP) utilizing coir and plastic fibers is examined. Beam samples of dimension 700 x 150 x 150 mm are placed in water tank for 28 days for curing, and the beam is marked with a grid to visualize precise crack distance. Beam samples are arranged in a simply supported condition and gauges are fixed to measure flexural strength with proper loading arrangement is utilized to complete the investigation. Fig. 6 shows the reinforcement details provided for the RCC beam samples utilized in this research.

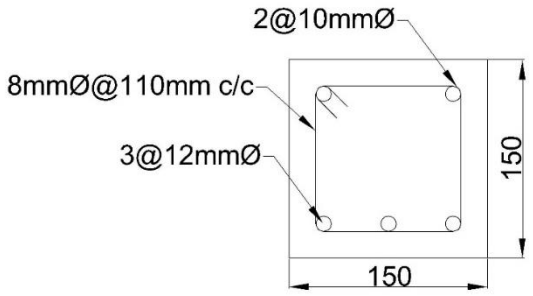

(a)

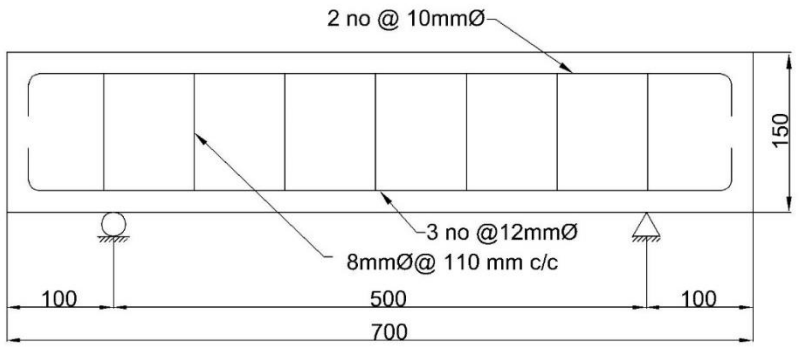

(b)

Fig. 6: Beam detailing

3. Results and Discussion

This section discusses the tests conducted for this research work. The detailed discussion is as follows:

3.1. Fresh Properties and Density of Concrete

Table 4 shows the fiber content of each concrete mix together with its workability and unit weight (UW). However, a superplasticizer dose of 0.5% was necessary for all combinations to achieve a design slump between 9 cm and 10.5 cm, which is important for efficiently pumping concrete. The fibers included in these new concrete mixes ranged widely, from artificial fiber like plastic to natural alternatives like coir. The range of fiber content levels to maintain a constant workability that was equivalent to the reference mix was 0.5% to 2.0%. The effectiveness of incorporating fibers into concrete formulations has been demonstrated by earlier studies, which also highlights the Fibers beneficial effects on performance.

The specimen's density was measured in accordance with code C-11249. The empty mould was first thoroughly oiled, then weighed, filled with concrete, and then weighed one more time. To calculate the wet density, the weight of the filled concrete (W_2) was subtracted from the weight of the empty weighed (W_1) mould and divided by the specimen volume (V_s). The density of concrete specimens (M1-0) is 2625.511 kg/m^3.

Table 4. Density of concrete specimens

Aspect ratio (17)	Coir Fiber				Plastic Fiber				Combined mix (coir +plastic)
	0.5%	1.0%	1.5%	2.0%	0.5%	1.0%	1.5%	2.0%	1.0%
Density (Kg/m^3)	2599	2573	2547	2520	2605	2586	2566	2547	2572
Slump (cm)	10.3	10.1	9.5	9.0	10.2	9.8	9.4	9.0	9.9

3.2. Compressive Strength

3.2.1 Compressive Strength for cubes

The M-40 concrete underwent compressive strength testing for varying durations, following the IS Code guidelines. The mean compressive strength of concrete for each mix and each day of curing was obtained from the arithmetic average of the compressive strength obtained from twelve specimens fabricated for every specific mix, and three specimens were cast on each corresponding day of curing. We present concrete mixes with a superplasticizer of 0.5% to achieve the M-40 target mean strength after 28 days. Fig. 7 shows that, in comparison with fiber mixtures, conventional concrete has the highest compressive strength. The compressive strengths of conventional concrete for 7 days, 14 days, 28 days, and 56 days are 38.5 MPa, 40.88 MPa, 50.66 MPa, and 53.55 MPa, respectively. The compressive strength of the concrete specimens was observed with the use of two types of Fibers (coir and plastic) mixed differently. Almost all the fibers carried compression strengths very close to each other, which will lead to not reaching the target strength in 28 days. The 1% and 1.5% concentration mixes of compressive strength have not achieved a strength of 35 MPa. The compressive strength of 2% coir fiber mix will not reach 20 MPa. Comparing mixtures with different fiber percentages, we found that the compressive strength dropped as the fiber percentage increased. Conversely, though a rise in early-age strength was noted. In particular, the higher fiber concentration of coir fiber could prevent the fiber and cement mixture from properly bonding. The reduction in compressive strength seen with increased coir fiber percentages in concrete mixes can be caused by a number of factors, including weaker fibers, inefficient bonding with the cement matrix, in the introduction of voids, and workability difficulties. The compressive strength of the plastic fiber mixes is nearly the same for 7 days, 14 days, 28 days, and 56 days with

values of 0.5% plastic fiber mix are 32.66 MPa, 34.22 MPa, 38.66 MPa, and 42.22 MPa respectively. The combined mix of 1% both coir and plastic fibers is 31.33MPa, 34.66 MPa, 37.77 MPa, and 42 MPa respectively. Because of Plastic fibers in concrete fail to achieve the target mean strength while maintaining constant compressive strength across mix percentages and testing durations. This is due to factors in their composition and behavior within concrete matrices. While plastic fibers enhance concrete's ductility and toughness, their mechanical properties may not be optimized for achieving the desired target strength, potentially due to limitations in the plastic material's tensile strength.

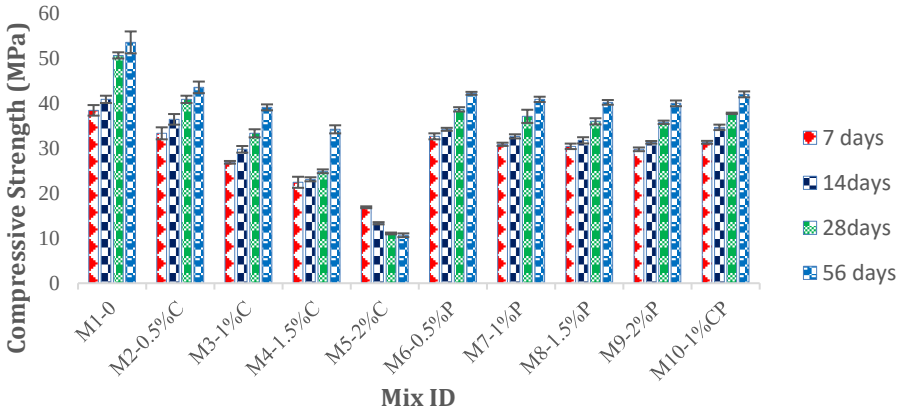

Fig. 7. Compression strength graph

3.2.2. Stress-Strain Behavior for Cylinder

The outcomes of the study, which was carried out over the course of 28 days on the nominal mix specimen and the optimized specimen (1% coir fiber and 1% plastic fibers). Fig. 8a presents the stress vs strain Load vs Deflection graphs for M1 & M10 providing comparative data. The stress-strain curve compares the performance of two concrete mixes, M1 and M10. M1 demonstrates higher stress values across the strain range compared to M10, indicating that M1 has greater strength and stiffness.

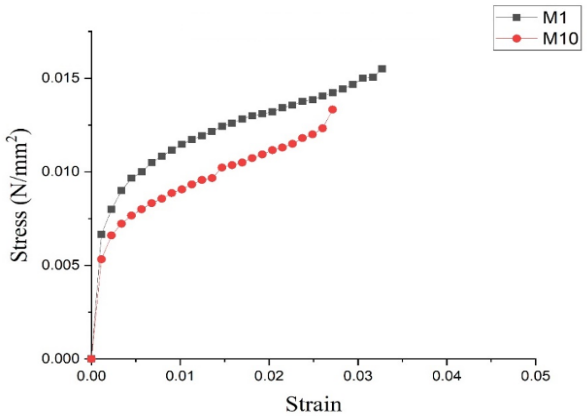

(a)

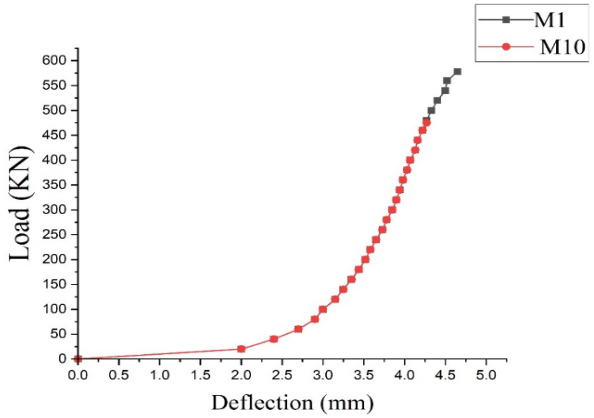

(b)

Fig. 8. Structural Behavior of M1 & M10 mixes

The curve for M10, represented by red dots, is consistently lower than M1's, suggesting that M10 deforms more easily under the same load. This could be due to different compositions or fiber additions in M10, which may reduce its load-bearing capacity and stiffness. The difference in curves highlights that M1 offers better mechanical properties under stress. Fig. 8b represents the load-deflection behaviour of two different materials, labelled M1 and M10. Both materials exhibit a non-linear relationship between load and deflection, indicating that they do not follow Hooke's law. The curve for M1 is steeper than that of M10, suggesting that M1 is stiffer and can withstand higher loads before reaching a certain deflection compared to M10.

3.3. Split Tensile Strength

Under code IS 5816, a split tensile strength test was performed for 7 days, 14 days, 28 days, and 56 days. The findings are shown in Fig. 9. The purpose of this test is to determine the tensile strength of concrete, which is critical for applications involving bending forces.

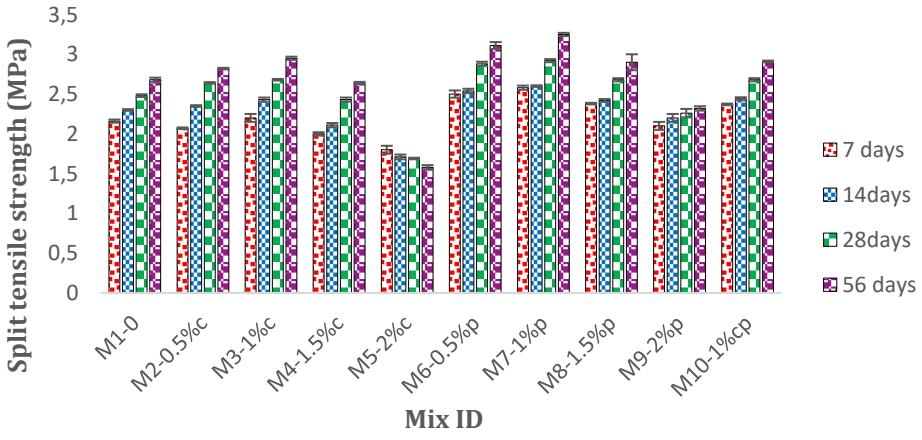

Fig. 9. Split tensile strength graph

It demonstrates how splitting plane tensile stresses can be applied to concrete while still maintaining its integrity, particularly in situations where higher durability is indicated by the tensile stresses. The split tensile strength of M3-1%C of the coir fiber used specimen is 2.95 MPa higher than the nominal mix of M1-0 split tensile strength of 2.68 MPa for the 56-day natural age curing period. The split tensile strength of M7-1%P of the plastic fiber specimen is increased to 3.25 MPa, M6-0.5%P is 3.11 MPa, and M8-1.5%P is 2.9 MPa when compared to nominal mix and coir fiber percentages. The split tensile strength of plastic fiber percentages of 0.5%, 1.0%, and 1.5% will increase while the age of curing will increase the strength is also increasing. The combined mix of both coir and plastic 1% is 2.91 MPa. The plastic fiber mixes strength will increase because ~~of~~ the plastic fiber made of synthetic polymers like polyester and polypropylene are used to create strong, durable plastic fibers. Their homogenous structure enhances tensile strength and provides excellent resilience to environmental deterioration, ensuring extended durability over time. Coir fibers, derived from coconut husk, are a natural substitute for artificial materials but may not match their tensile strength due to natural oscillations in the fiber structure. They also pose challenges for certain processing and treatment techniques and may deteriorate over time due to exposure to moisture, making them less durable.

3.4. Flexural Strength

The results of the Flexural strength tests performed on the concrete specimens are shown in the Fig. 10. Flexural strength findings for all types of fiber mixtures show good results when compared to the nominal mix and comparing the results between coir fiber and plastic fiber. The flexural strength of M3-1%C of the coir fiber used in the specimen is 7.95 MPa higher than the nominal mix of M1-0. The flexural strength was 6.21 MPa for the 56-day natural age curing period. The split tensile strength of M7-1%P of the plastic fiber specimen is increased to 9.48 MPa, M6-0.5%P is 9.16 MPa, M8-1.5%P is 8.94 MPa, and M9-1.5%P is 8.56 MPa when compared to nominal mix and coir fiber percentages. The flexural strength of plastic fiber percentages of 0.5% to 2% will increase while the age of curing will increase. The combined mix of both coir and plastic 1% is 7.58 MPa. The flexural strength got increased because plastic fibers are strong and durable due to their uniform structure and resistance to environmental deterioration. In contrast, coir fibers obtained from coconut husks have inherent structural differences and are less resistant to moisture, resulting in reduced tensile strength and durability.

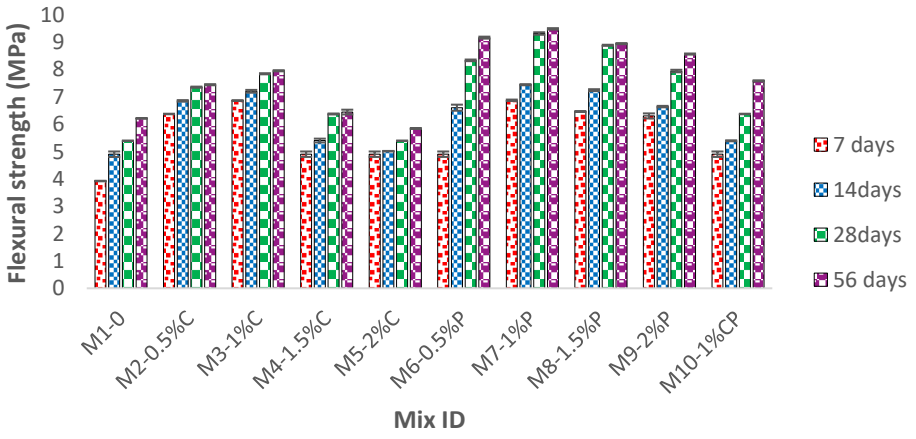

Fig. 10. Flexural strength graph

3.6 Durability properties

For this experiment on fiber-reinforced concrete using coir and plastic fibers, assessing the durability properties of the concrete is crucial. The following durability properties will be evaluated:

3.6.1 Water Absorption

One of the most important factors influencing concrete long-term performance and durability is water absorption. Concrete absorbs water via pore structure and capillary action; the amount of absorption is determined by several parameters such as ingredient quality, porosity, curing conditions, and mix design. Because of variations in moisture content, high water absorption can shorten lifespan, raise the danger of corrosion, and alter dimensions. Effective curing and mix design are two strategies to reduce water absorption. The long-term performance and structural integrity of concrete depend on the efficient regulation of water absorption. The test results of water absorption in every combination are shown in the Fig. 11. The water absorption percentages for various concrete mixes with different compositions of coir fiber ("C") and plastic fiber ("P") at 28 and 56 days of curing. Overall, most mixes show an increase in water absorption from 28 to 56 days, indicating that permeability may rise over time, possibly due to changes in the concrete's microstructure or fiber interactions. The M1-0, likely a control with no added fibers, has relatively low water absorption at both ages, suggesting a denser and less permeable matrix. In contrast, mixes containing coir fiber the percentage of coir fiber is adding to concrete it exhibit higher water absorption, especially at 56 days, indicating that increasing coir fiber content could lead to higher porosity, allowing more water ingress over time. This could be due to the natural characteristics of coir fiber, which may create additional voids or pathways in the concrete matrix.

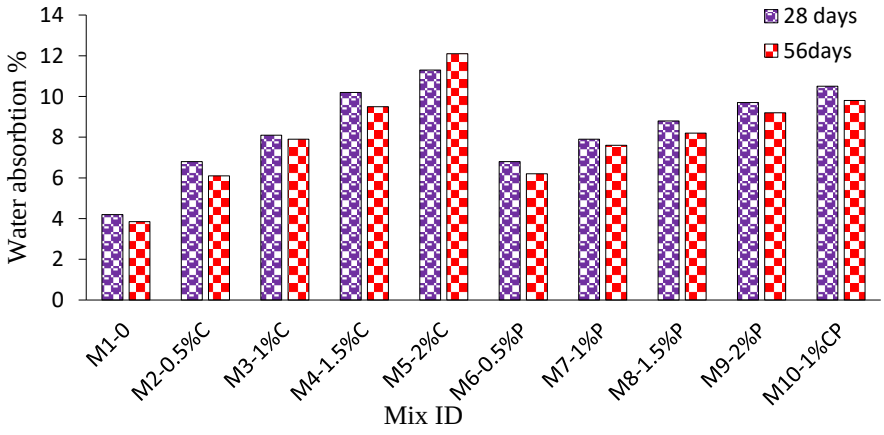

Fig. 11. Water absorption with respect to design mixes

On the other hand, mixes that include plastic fiber alone or in combination with coir fiber, like M6-0.5%P to M10-1%C&P, generally display lower water absorption. This suggests that plastic fiber may help reduce permeability, possibly by reinforcing the matrix or filling voids more effectively. The effect is particularly evident in mixes with lower coir and balanced plastic fiber content, where water absorption remains lower, even at 56 days. This observation indicates that plastic fiber might enhance durability by reducing the concrete's porosity and resistance to water absorption. For the applications where low water absorption and durability are critical, mixes with reduced coir fiber content or a combination of plastic and coir fibers appear beneficial. These compositions exhibit

improved resistance to water ingress, potentially reducing issues related to chemical attack, and steel corrosion over the structure's lifespan.

3.6.2. Water Permeability

The graph shows the water penetration depth for various concrete mixes, each containing different proportions of coir fiber ("C") and plastic fiber ("P"). This measurement reflects the concrete's resistance to water ingress, with lower penetration depths indicating better water resistance and durability. Significant variation in penetration depth across the mixes reveals that the type and proportion of fibers greatly influence permeability. Mixes with higher amounts of coir fiber, such as M5-2%C, exhibit the deepest water penetration (around 100 mm), suggesting that higher coir content increases porosity, allowing more water to penetrate and potentially reducing durability. In contrast, mixes containing plastic fiber, like M6-0.5%P and M7-1%P, display notably lower penetration depths, with M6-0.5%P having a penetration depth below 40 mm. This indicates that plastic fibers help to reduce permeability, likely by filling voids and creating a denser matrix that hinders water movement.

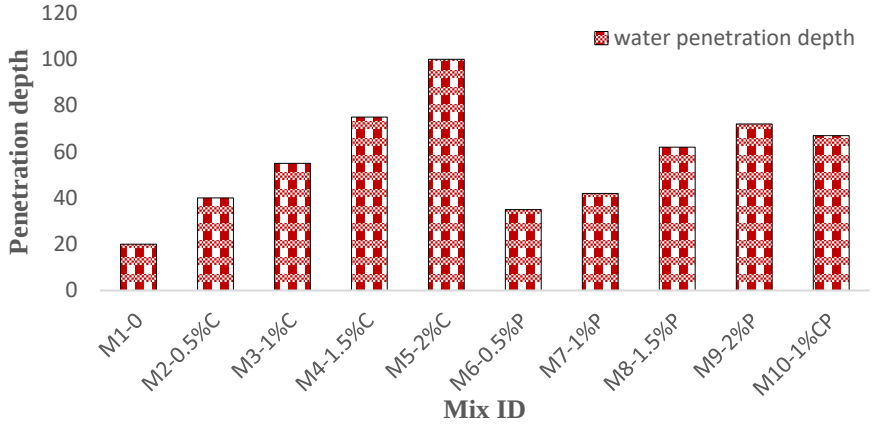

Fig. 12. Water penetration depth for design mixes

Table 5. Concrete permeability

Mix ID's	Permeability Coefficient, K (m/s)
M1-0	3.108×10^{-12}
M2-0.5%C	1.243×10^{-11}
M3-1%C	2.351×10^{-11}
M4-1.5%C	4.371×10^{-11}
M5-2%C	7.772×10^{-11}
M6-0.5%P	9.520×10^{-12}
M7-1%P	1.370×10^{-11}
M8-1.5%P	2.987×10^{-11}
M9-2%P	4.029×10^{-11}
M10-1%CP	3.488×10^{-11}

Mixes that combine both coir and plastic fibers, such as M10-1%C&P, show intermediate penetration depths, suggesting that plastic fibers can offset the increased permeability associated with coir fiber to some extent. Overall, the control mix M1-0, which likely contains no fibers, has one of the lowest penetration depths, showing that a standard

concrete matrix may have better water resistance than those with high coir content. In terms of durability, mixes with lower penetration depths particularly those with plastic fiber or balanced fiber content—are preferable, as they are more resistant to moisture-related damage, including reinforcement corrosion and freeze-thaw cycles. For applications needing high durability, mixes with plastic fiber alone or a lower proportion of coir fiber are recommended due to their reduced water permeability. The permeability coefficient is shown in Table 5, calculated using Darcy's law, provides valuable insights into concrete quality and suitability for various applications. Fig. 12 presents graph for water penetration depths for different mixes.

3.6.3. Acid Attack (H_2SO_4)

This exposure allows researchers and engineers to evaluate the performance of the concrete under conditions of chemical attack, assessing factors such as degradation, mass loss, surface roughness, and changes in mechanical properties. When curing concrete in acidic conditions, compressive strength and density decrease, particularly noticeable in exposed aggregates prone to acid corrosion. Immersing concrete cubes in acid solutions significantly reduces their compressive strength compared to standard curing. Acid attacks intensify with higher cement proportions, targeting hydrated lime and weakening the bond between cementitious aggregates, leading to mass loss and decreased durability.

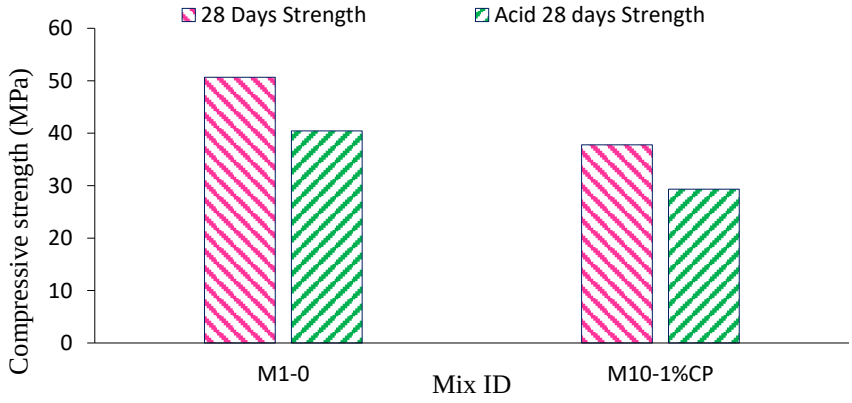

Fig. 13. Compressive strength graph for Acid attack (H_2SO_4)

Fig. 13 illustrates the graph of compressive strength for sulfuric attack of two concrete mixes, M1-0 and M10-1%CP, under different conditions at 28 days. The M1-0 mix serves as the reference mix, while M10-1%CP includes a 1% addition of coir-plastic (CP) fibers. The results reveal that the M1-0 mix achieves a higher compressive strength compared to M10-1%CP under standard conditions, suggesting that the addition of 1% CP fibers slightly reduces compressive strength. This reduction might indicate that, at a low content level, CP fibers do not significantly contribute to compressive strength. Both mixes exhibit a decrease in compressive strength after exposure to acid, which aligns with expectations, as acid exposure generally weakens concrete. Interestingly, the relative reduction in strength due to acid exposure is similar between the two mixes, implying that the inclusion of CP fibers does not notably enhance acid resistance at this 1% level.

3.6.4 Sulfate Attack ($MgSO_4$)

Researchers can assess deterioration, mass loss, surface roughness, and mechanical property changes in concrete thanks to this corrosive action. Comprehending the influence of magnesium sulphate on the longevity of concrete is essential for enhancing mix designs,

choosing suitable building materials, and putting preventive measures in place against degradation. In sulfate-rich settings, this aids in the development of strong infrastructure solutions for long-term performance and safety. Sulphates react with the calcium-silicate-hydrate gel in concrete, causing the gel to disintegrate and impair the cohesiveness of the material. Ettringite crystals are produced throughout this procedure. and push on the paste, producing fissures and affecting structural integrity. Concrete loses strength due to major changes in its chemical and physical characteristics. Following exposure to the magnesium sulfate solution, all of the concrete sample displayed deterioration.

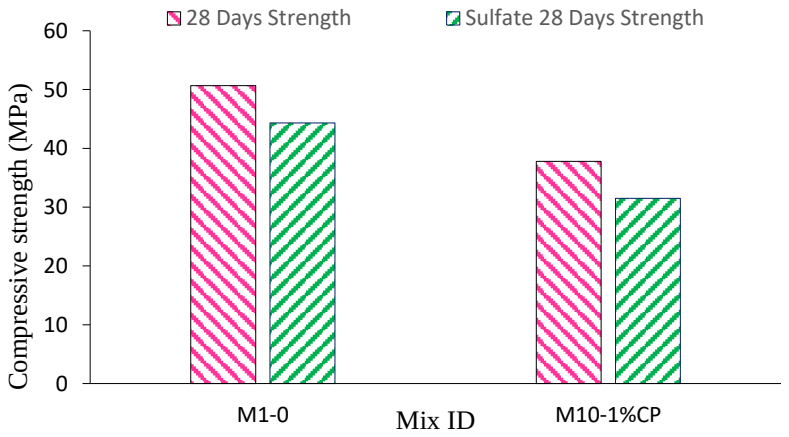

Fig. 14. Compressive strength graph for Sulfate attack ($MgSO_4$)

Fig. 14 displays the presents graph of compressive strength for sulfate attack ($MgSO_4$) of two concrete mixes, M1-0 and M10-1%CP, at 28 days under standard conditions and after sulfate exposure. M1-0, the reference mix, shows higher compressive strength compared to M10-1%CP under both conditions, indicating that adding 1% coir-plastic (CP) fibers slightly reduces compressive strength. Both mixes experience a drop in strength after sulfate exposure, as expected due to sulfate's corrosive effects on concrete. However, the reduction in strength is similar in both mixes, suggesting that 1% CP fiber content does not significantly enhance sulfate resistance. Thus, optimizing fiber content or other mix adjustments may be necessary to improve durability against sulfate exposure.

3.7. Microstructural Analysis

Microstructural analysis of the fiber-reinforced concrete using coir and plastic fibers will involve examining the internal structure of the concrete at the microscopic level. This analysis helps to understand the interaction between the fibers and the cement matrix, the distribution and orientation of the fibers, and the overall impact on the concrete's mechanical properties. The following techniques will be employed:

3.7.1. Scanning Electron Microscopy (SEM)

The SEM image reveals the microstructure of concrete, showcasing key components like C-S-H gel, Ca $(OH)_2$, and unreacted silica. The dense C-S-H gel indicates good hydration and potential strength. However, the presence of voids and unreacted materials might impact the concrete's long-term durability and permeability. Further analysis is needed to fully assess the material's properties. At this high magnification, we can observe individual particles and their interconnections.

Fig. 15 and 16 shown the SEM images of the normal mix (M1) show a dense microstructure with some porosity at high magnifications, indicating good strength and durability, though

the porosity may affect permeability and degradation resistance. Particle distribution is generally uniform, but some agglomeration could impact homogeneity and mechanical properties

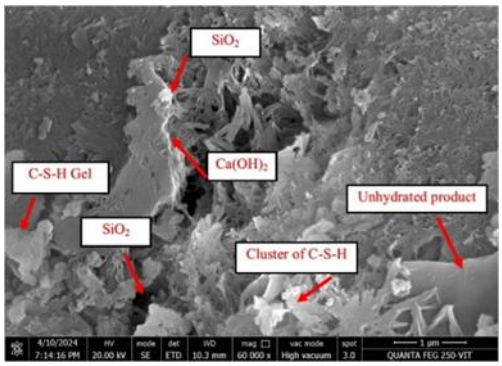

(a) SEM image at 20 kv, 60000 x

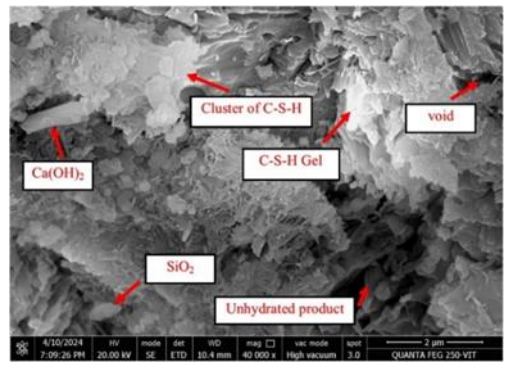

(b) SEM image at 20 kv, 40000 x

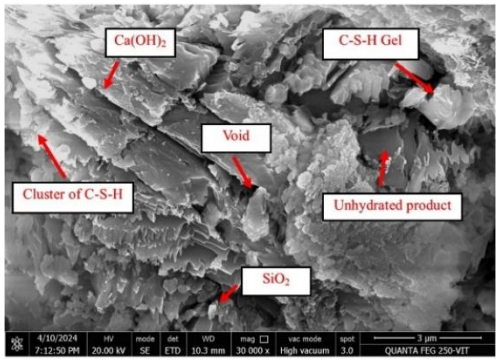

(c) SEM image at 20 kv, 30000 x

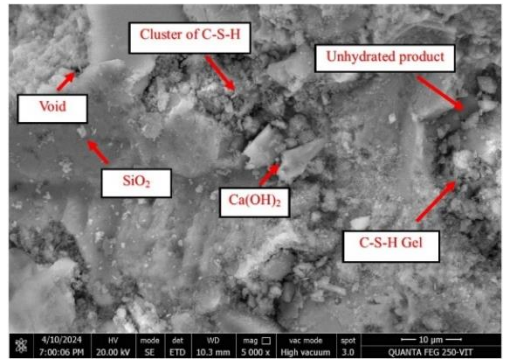

(d) SEM image at 20 kv, 5000 x

(e) SEM image at 20 kv, 20000 x

Fig. 15. SEM image for normal mix (M1)

Larger pores observed at lower magnifications may influence strength and durability under cyclic or harsh conditions. Overall, the mix has a relatively uniform particle arrangement with interlocked particles, suggesting strong mechanical properties. Further analysis and comparisons with other mixes would help assess the material's performance

in specific applications. For the concrete samples M1 and M10 SEM analysis was carried out. In the analysis process, it is observed C-S-H Gel was arranged in cluster which shows interfacial transition zone for these two mixes are strong which concludes this sample shows good strength.

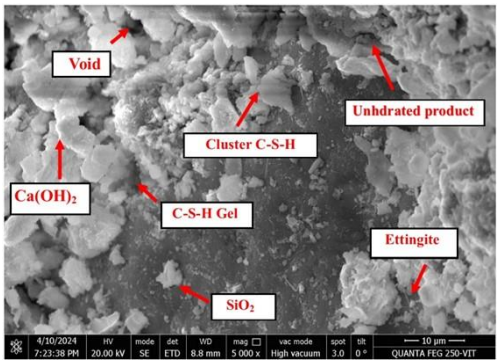

(a) SEM image at 20 kv, 5000 x

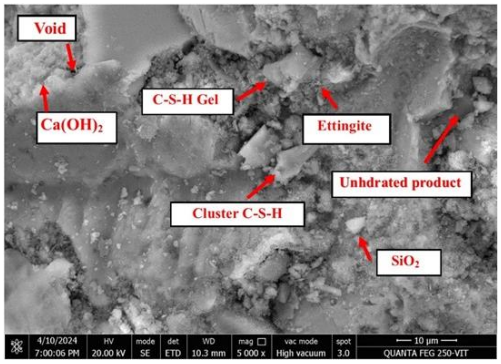

(b) SEM image at 20 kv, 5000 x

(c) SEM image at 20 kv, 10000 x

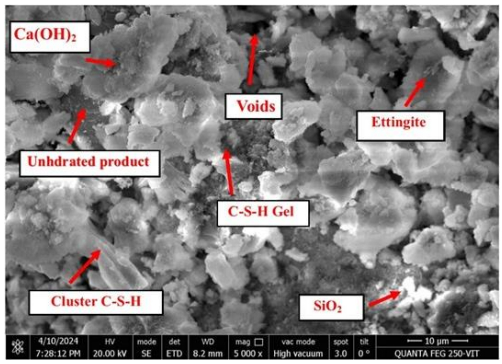

(d) SEM image at 20 kv, 5000 x

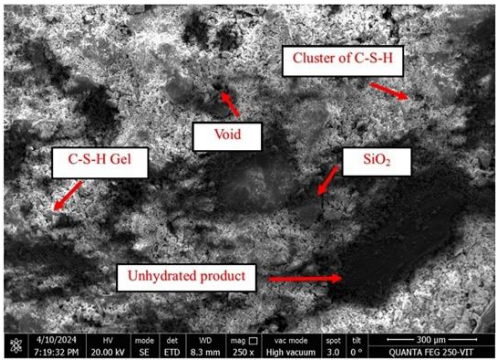

(e) SEM image at 20 kv, 250 x

Fig. 16. SEM image for optimized mix (M10)

3.7.2. Energy Dispersive X-Ray (EDX)

Microstructure analysis of EDX is shown in the below Fig. 17 a & b. The presence of calcium, aluminum, silicon, carbon, and oxygen was found using EDS analysis in the research of fiber concrete. The EDS analysis of fiber-reinforced concrete reveals key elements such as calcium, aluminium, silicon, carbon, and oxygen, which are integral to the material's

composition and its interaction with reinforcing fibers. Calcium (Ca) is a major component of cement and forms calcium silicate hydrates (C-S-H), which provide the primary binding strength. Aluminium (Al) contributes to the formation of calcium aluminate hydrates (C-A-H), improving early strength and durability. Silicon (Si) combines with calcium to form C-S-H, further strengthening the concrete. Carbon (C) is present from reinforcing carbon fibers or carbon-based additives, while oxygen (O) plays a vital role in the hydration process and the formation of C-S-H.

The detection of these elements through EDS confirms the presence of the typical concrete constituents and their interaction with fibers, particularly highlighting the incorporation of carbon fibers into the matrix. To optimize the performance of fiber-reinforced concrete, further research should focus on the distribution and orientation of fibers, the fiber-matrix interface, and the microstructural analysis. These factors influence load transfer, mechanical properties, and durability, which are crucial for achieving improved strength, ductility, and overall performance. Fig. 17 c and d shows EDS covered image for M1 and M10 mixes. In order to offer comprehensive insights into material composition and support microstructural investigation and quality evaluation, this technique combines electron microscopy with X-ray analysis. When combined with microstructural characteristics, the resulting "EDS layered image" helps to facilitate spatial comprehension and association with elemental composition. Electron images are shown in Fig. 17 e and f

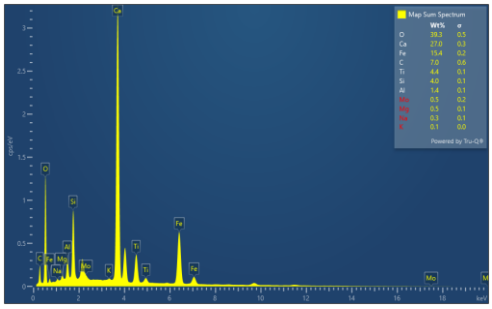

(a) EDX image showcasing properties of ingredients of nominal mix (M1)

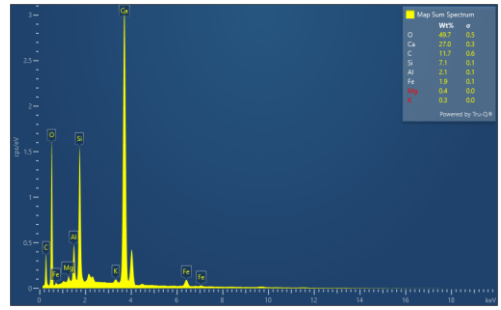

(b) EDX image showcasing properties of ingredients of optimized mix (M10)

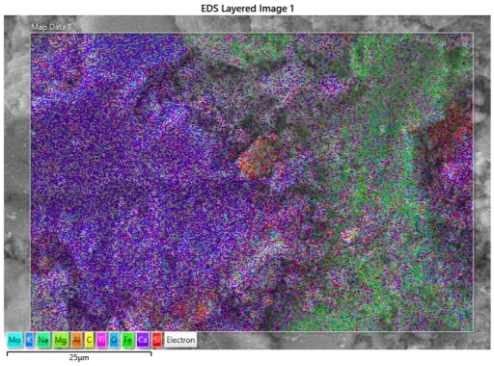

(c) EDS image at 25microns for nominal mix (M1)

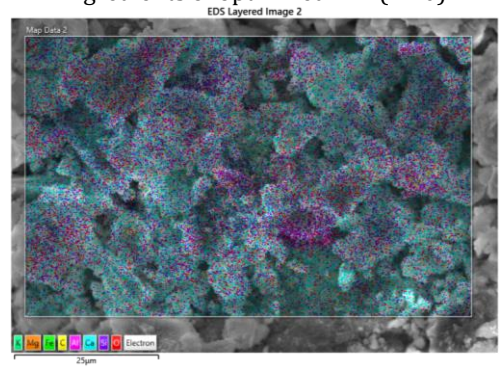

(d) EDS image at 25microns for optimized mix (M10)

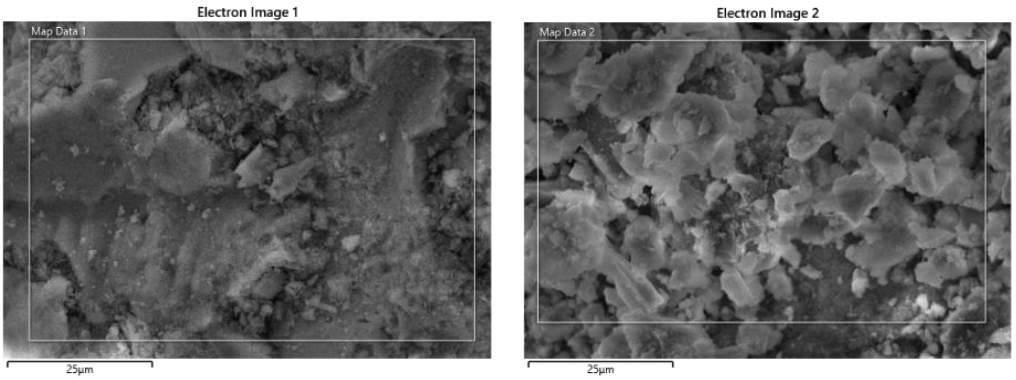

(e) Electron image at 25 microns for nominal mix (M1)

(f) 20 Electron image at 25 microns for optimized mix(M10)

Fig. 17: EDX, EDS & Electron images for nominal mix (M1) and optimized mix(M10)

3.7.3. Fourier Transform infrared Spectroscopy (FTIR)

The FTIR spectra of different concrete mixes with varying percentages of carbon fiber (C) and polypropylene fiber (P) reveal key insights into the chemical composition and molecular structure of the materials. The spectra show a general trend of increasing transmittance with rising wavenumbers, typical for concrete materials. The addition of carbon and polypropylene fibers has minimal impact on the overall spectral features, though slight variations in peak intensities and positions suggest potential changes in fiber distribution, fiber-matrix interface, and concrete microstructure.

These FTIR results indicate that the fibers do not significantly alter the fundamental chemical composition of the concrete, but their presence might influence the microstructure and bonding mechanisms, as seen in the variations of peak intensities. Further analysis, such as quantitative peak intensity measurements, and correlation with mechanical properties, would provide a clearer understanding of how fiber addition affects the concrete's performance. Combining FTIR with techniques like SEM and EDS can offer a more comprehensive view of the material's structure and properties.

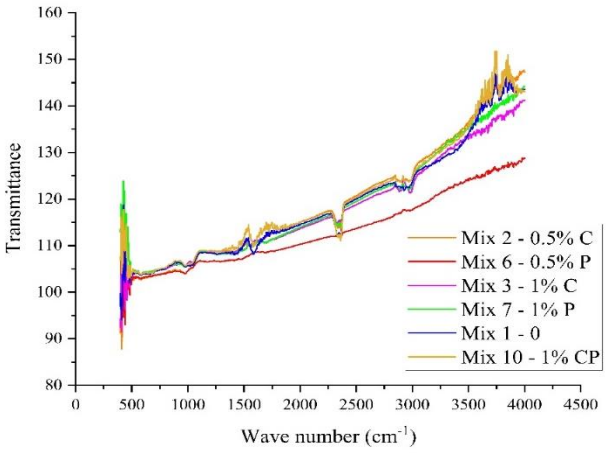

Fig.18. FTIR analysis graphs for all concrete mixes

It is applicable in a wide range of fields, including chemistry, materials science, pharmacology, and forensic investigation. It supports both qualitative and quantitative examinations of both organic and inorganic compounds. FTIR is a mainstay in analytical chemistry and materials research because of its reputation for sensitivity, rapidity, and non-destructiveness. Microstructure analysis of FTIR is shown in the below Fig. 18

3.7.4. Interfacial Transition Zone

Interfacial Transition Zones (ITZs), aggregates, cement matrix, COIR fiber, and plastic fiber constitute fiber-reinforced composite (FRC), a non-homogeneous material with four distinct phases. The mechanical properties of this material on a macroscopic scale are intricately linked to its microstructure. Consequently, a thorough investigation into the microstructures of the cement paste-aggregate and cement paste-steel fiber ITZs is imperative. To facilitate this investigation, ten samples were meticulously prepared for microscopic imaging tests, designated as M1 (Nominal Mix), M2 (0.5%C), M3 (1.0%C), M4 (1.5%C), M5 (2%C), M6 (0.5%P), M7(1%P), M8 (1.5%P), M9(2%P), AND M10 (1%CP). The manufacturing process of these using microscopic samples is clarified in Fig. 17, all samples were meticulously crafted prior to any loading, ensuring that the test results accurately portray the initial morphology of the interfacial transition zone.

3.7.4.1. ITZ at fiber-cement paste and aggregate-cement paste

The study examines the microstructure of the Interfacial Transition Zones (ITZ) between the aggregate and cement paste in M1. The ITZ between the fiber and mortar matrix in specimens M2 to M5. The matrix is firmly bonded to the coir and plastic fiber, and the cement composite around the fibers is sufficiently hydrated. Dense ITZs and harmful crystals are observed on the fiber surface, but a small amount of microcracks exist in the transition zone. In specimens M6 to M10, the fiber surface is covered with a small number of harmful crystals, and the fibers are smoother with fewer cracks. The ITZ thickness of the fibers and mortar matrix is small, and the content of fibers has a small effect on ITZs. A distinct interfacial transition zone is generated between the fiber and matrix, resulting in a compact interfacial transition zone around the fiber in Fig. 19. The microstructural image of the all-concrete mix, which incorporates coir fiber, reveals several important features that contribute to the properties of the composite. Aggregates are visible within the matrix, providing bulk and contributing to the mix's mechanical strength, while the calcium-silicate-hydrate (C-S-H) phase, crucial for binding, can be seen surrounding these aggregates. Coir fibers, embedded within the mix, play a significant role in enhancing toughness by bridging microcracks and helping to reduce stress concentrations. The Interfacial Transition Zone (ITZ), situated between the aggregates and the cement paste, appears to be less porous in this fiber-reinforced mix.

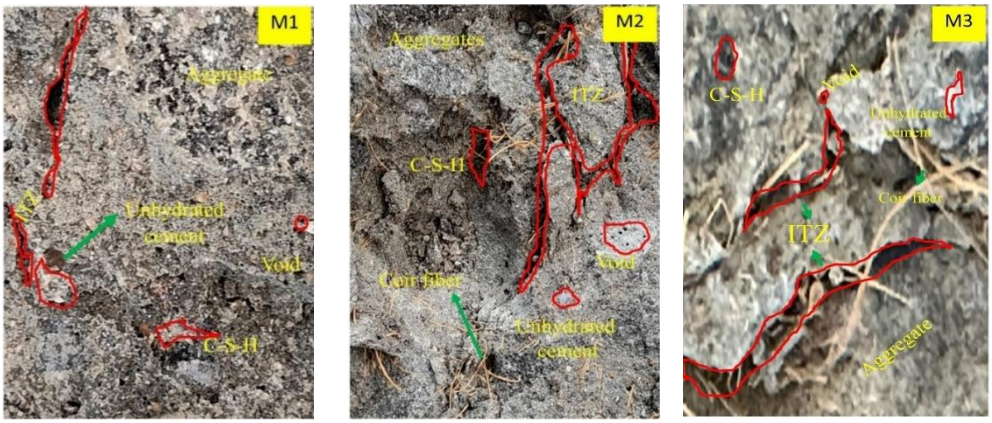

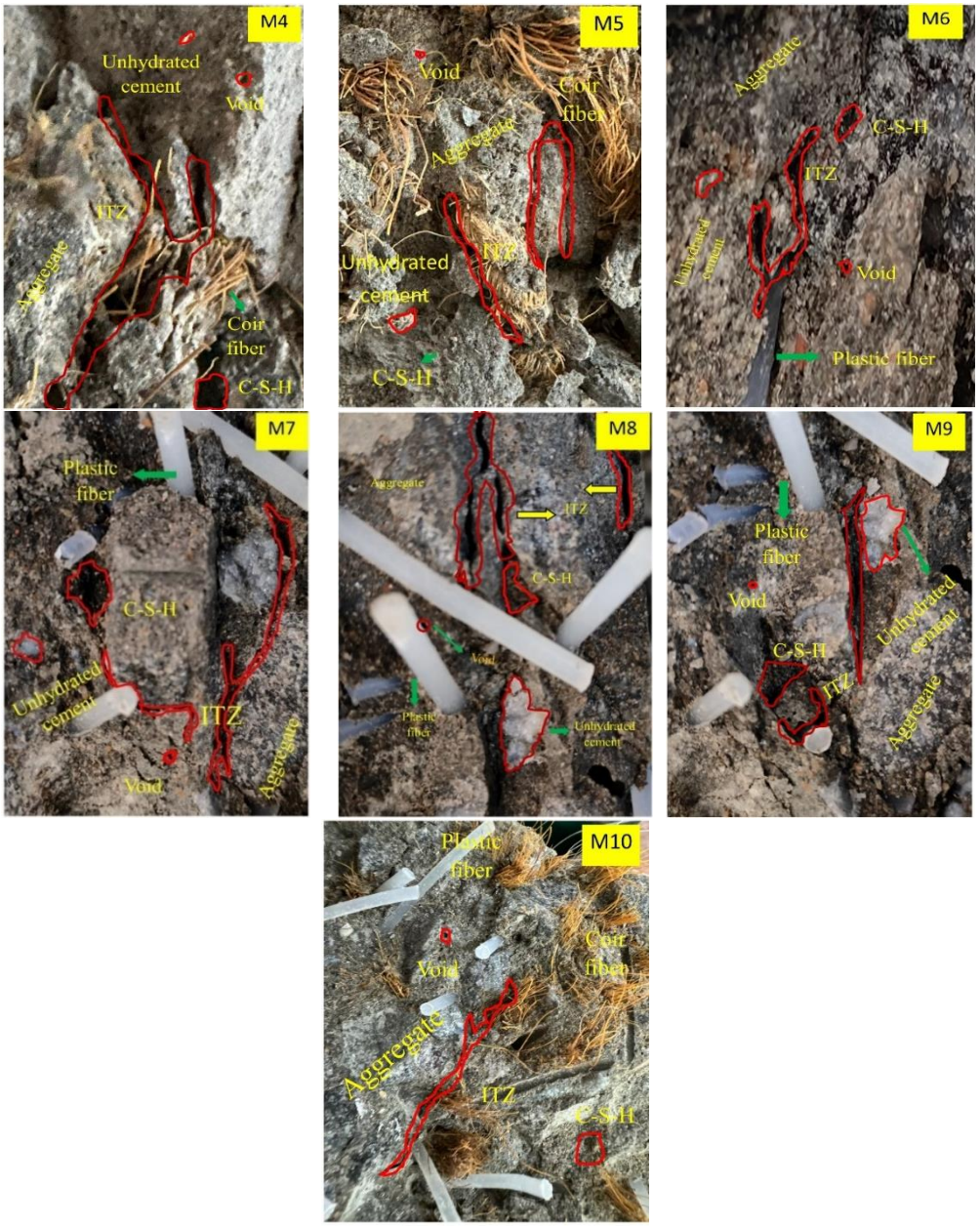

Fig. 19. ITZ images for different mixes

The addition of coir fibers seems to improve the ITZ quality, likely by minimizing voids and reducing microcracking around the aggregate-matrix interface, resulting in stronger bonding. However, some unhydrated cement particles are still present, indicating incomplete hydration, which could be due to limited water or mixing conditions and might slightly impact the concrete's strength. Although voids are present, the distribution appears more controlled due to the coir fibers, which help reduce crack propagation.

3.8. Flexural Behavior of Beams

From Fig. 20a presents the experimental configuration for flexural strength test and observed crack pattern of B1-0. In Fig. 20b support conditions are clearly shown for B2-1%C with observed crack patterns. Fig. 20c depicts the crack patterns observed on the B3-1%P with support condition. In Fig. 20d crack patterns of B4-1%CP is shown. For B5-1%CP, Fig. 20e shows the observed crack pattern. From the above Fig. 20, It has been noted that the crack patterns vary for reinforced and non-reinforced samples. In reinforced and non-reinforced concrete beams, crack behaviour differs significantly due to the presence of reinforcement.


(a) Beam setup for B1-0


(b) Beam setup for B2-1%C


(c) Beam setup for B3-1%P

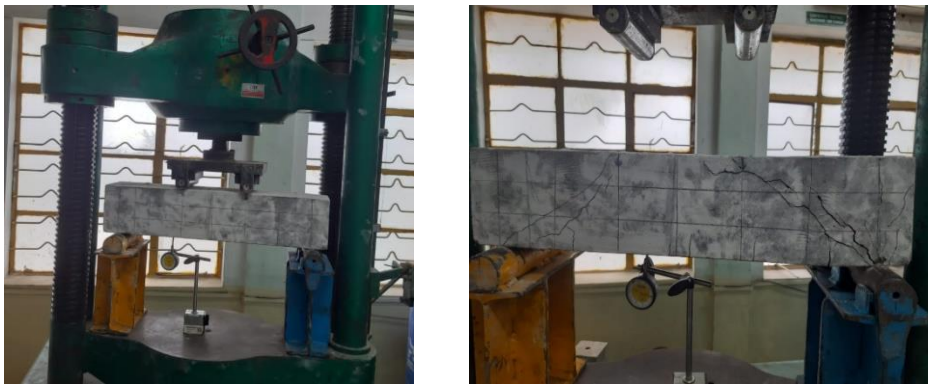

(d) Beam setup for B4-1%CP

(e) Beam setup for B5-1%CP

Fig. 20 Experimental setup and crack patterns for Beams (B1, B2, B3, B4, and B5 mixes)

In non-reinforced beams, cracks initiate at stress concentration points, such as corners or edges, and propagate rapidly along paths of least resistance, resulting in an irregular and unpredictable crack pattern. This often leads to an abrupt, brittle failure due to the uncontrolled crack progression. In the reinforced beams exhibit more controlled crack initiation, with the reinforcement restraining crack width and propagation. Consequently, the cracks in reinforced beams are finer, more evenly spaced, and aligned with the reinforcement direction, contributing to a more predictable crack pattern. This controlled cracking and gradual failure mode provide the beam with a ductile failure mechanism, allowing for greater deformation and warning before ultimate failure. Factors such as material properties, loading conditions, and reinforcement details impact crack patterns. For instance, overloading, design deficiencies, or environmental degradation can lead to cracking in reinforced beams, but these cracks are typically limited by the reinforcement, which provides additional load-carrying capacity. Observing crack patterns, especially in the tension zone where the cracks concentrate, and inspecting the exposure of reinforcement can reveal essential information about structural health. Therefore, understanding and monitoring crack behaviour are critical for designing durable structures, conducting inspections, and performing maintenance to ensure long-term structural serviceability.

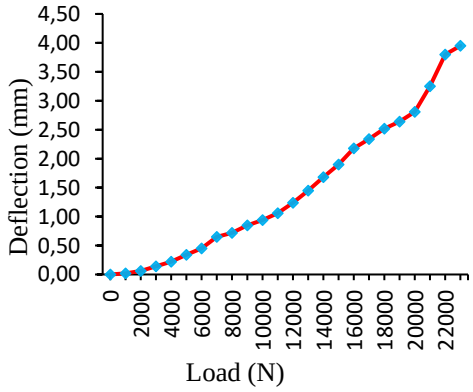

(a) load vs deflection graph for B1-0

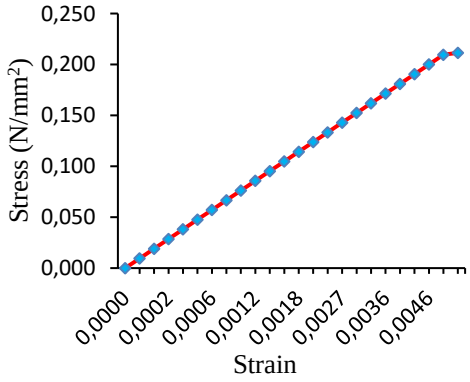

(f) stress vs strain graph for B1-0

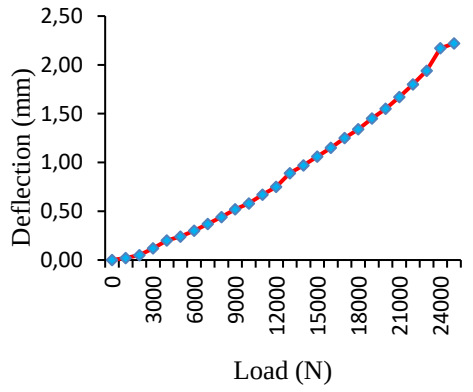

(b) load vs deflection graph for B2-1%C

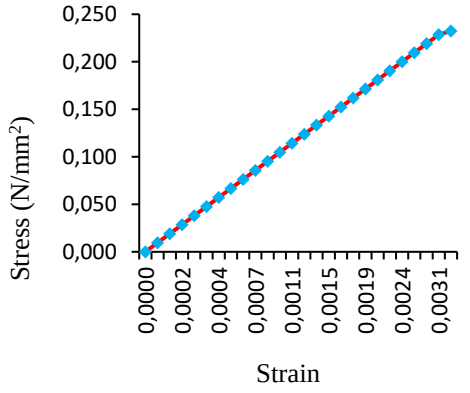

(g) stress vs strain graph for B2-1%C

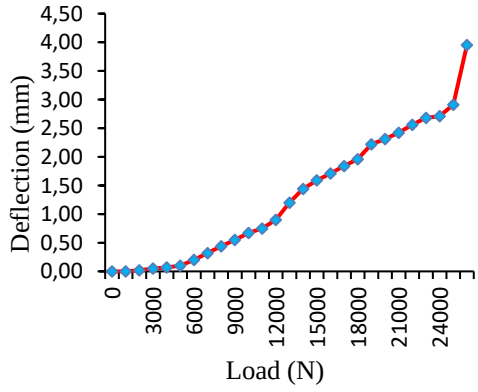

(c) load vs deflection graph for B3-1%P

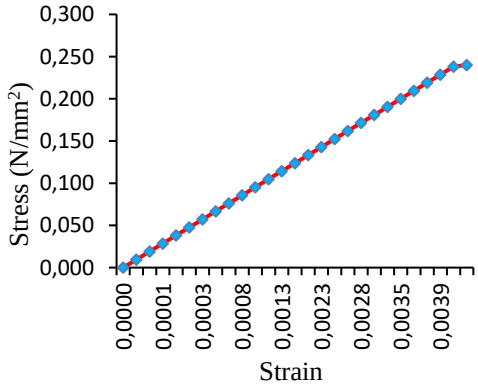

(h) stress vs strain graph for B3-1%P

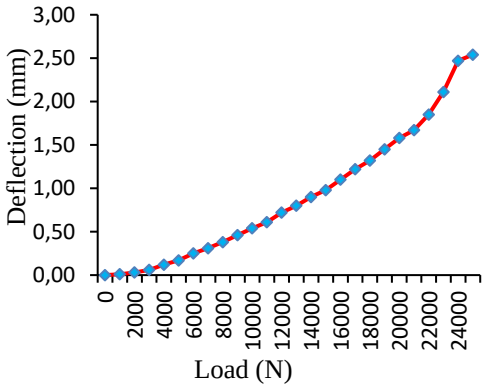

(d) load vs deflection graph for B4-1%CP

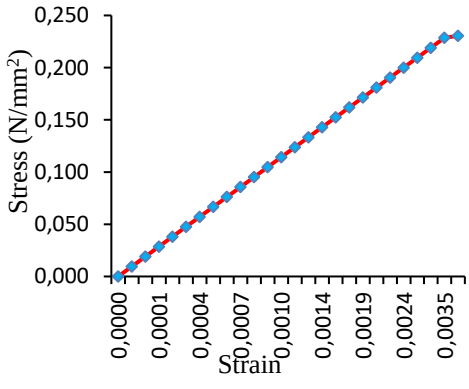

(i) stress vs strain graph for B4-1%CP

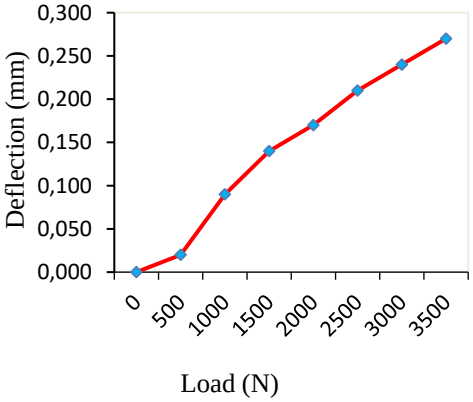

(e) load vs deflection graph for B5-1%CP

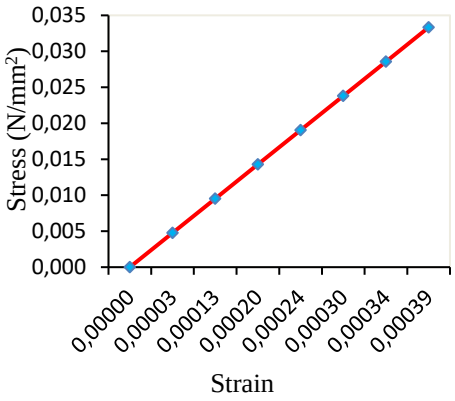

(j) stress vs strain graph for B5-1%CP

Fig. 21. Load table vs Deflection and Stress vs Strain graphs

Fig. 21 shows the load vs deflection and Stress vs Strain graphs; it represents the flexural strength of B1-0 of 3.288 MPa for 28 days of natural curing. The flexural strength of B2-1%C is 3.61 MPa, B3-1%P is 3.73 MPa, B4-1%CP is 3.58 MPa, and B5-1%CP is 0.6 MPa. The above sentence state that B1, B2, B3, and B4 are cast with reinforcement, and B5 beams are cast with reinforcement-free. While comparing each mix, the plastic fibers added to concrete is higher than coir, and coir is superior to the nominal mix. The comparison of B5 and B1 to reduce the 84.22% of steel was reduced. Optimized mix of B4 also gives better strength than nominal mix. While adding fibers to the concrete, the compressive strength of the concrete was reduced compared to the nominal mix. Comparing mixtures with different fiber percentages, we found that the compressive strength dropped as the fiber percentage increased.

4. Conclusion

This study examined the consequences of coir and plastic fibers the mechanical characteristics, durability properties, microstructural study, and structural applications of Fiber reinforced concrete by evaluating experimental results. From the results got, the following conclusions are as follow.

- While adding fibers to the concrete, the compressive strength of the concrete ~~was~~ reduced in fiber mix of M2-0.5%C and M6-0.5%P by 25.9% at 28 days and 29.96% at 56 days age of curing, the strength decreases when compared to the nominal mix of M1-0. The strength decreases in fiber mix of M2-0.5%C and M6-0.5%P 34.12% at 28 days, and 27.5% at 56 days age of curing compared to the nominal mix of M1-0 Comparing mixtures with different fiber percentages, we found that the compressive strength dropped as the fiber percentage increased. Conversely, however, a rise in early-age strength was noted. In particular, the higher fiber concentration fiber and cement mixture has improperly bonding. It caused by a number of factors, including weaker fibers, inefficient bonding with the cement matrix, the introduction of voids, and workability difficulties. when compare to individual fiber mixes optimized mix strength are better.
- The split tensile strength was increased in the concentration of 1% mixes of both coir and plastic fibers when compared to the nominal mix. The coir fiber mixes of M3-1%C of 8% at 28 days and 10% at 56 days of curing, the strength will increase than normal mix M1-0. For the plastic fibers of M7-1%P was 17.7% at 28 days and 21.2% at 56 days will increase the strength than normal mix. When compared to coir fiber and plastic fiber, the plastic fiber strength increases of M7-1%P by 9%.
- Flexural strength was increased in the concentration of 1% mixes of both coir and plastic fibers when compared to the nominal mix. The coir fiber mixes of M3-1%C of 45% at 28 days and 28% at 56 days of curing, the strength will increase than normal mix M1-0. For the plastic fibers of M7-1%P was 72% at 28 days and 52% at 56 days will increase the strength than normal mix. In the comparison between fibers the concentrations of plastic fiber will give better strength than coir fiber concentrations. The strength increases of plastic fiber of M7-1%P by 30%, because the plastic fiber has strong and durable in nature due their uniform texture and it has flexible in nature than coir fiber.
- The optimized concentration of M10-1%CP the strength increased by 20% than normal mix M1-0. The optimizes mix will give good mechanical performance by effectively strengthening the link between fiber to fiber it has meshing the components with concrete. It provides a stronger tensile bond than nominal mix.
- The SEM analysis shows the coir and plastic fiber with porous structure and it bonded strongly with the concrete matrix. It resulting the better mechanical characteristics.
- The EDS shows the optimizes mix had a lower Calcium/Silicon (Ca/Si) and Sodium/Titanium (Na/Ti) than nominal mixture, indicating the higher mechanical strength results good C-S-H gel formation. EDX investigation revealed the properties in concrete.
- The results of FTIR indicated that the good molecular structure and it indicates the carbonation bonding in fiber reinforced concrete, it enhancing the strength characterizes of mixes.
- The ITZ shows the effectiveness of concrete concentration the surface layer laminated with voids, week hydration products as C-S-H.
- The fiber reinforced concrete beams give good flexural strength compared to nominal mix.
- The study highlights the potential of using waste fibers into the concrete mixes to promote sustainability goals, while considering specific applications requirements.

The study's conclusions suggest that adding of 1% of coir and plastic fibers enhances the mechanical performance of concrete. These investigation shows that the concrete reinforced with fibers is promising for creating sustainable concrete structures.

5. Acknowledgements

The author would like to express gratitude for the help that was provided by the civil engineering department, faculty and staff at KL University, Vaddeswaram.

References

[1] Chen L, et al. Recent developments on natural fiber concrete: A review of properties, sustainability, applications, barriers, and opportunities. Dev Built Environ. 2023;16:100255. https://doi.org/10.1016/j.dibe.2023.100255
[2] Ja'e IA, et al. Experimental and predictive evaluation of mechanical properties of kenaf-polypropylene fibre-reinforced concrete using response surface methodology. Dev Built Environ. 2023;16:100262. https://doi.org/10.1016/j.dibe.2023.100262
[3] Akinpelu MA, Salman AS, Jimoh YA, Yahaya IT, Salami HM. Impact of treatment temperature of metakaolin on strength and sulfate resistance of concrete. Res Eng Struct Mater. 2024;x(x):1-19. https://doi.org/10.17515/resm2024.06ma1012rs
[4] Kumar RV, Prabaghar A. Evaluation of strength of self-compacting concrete having dolomite powder as partial replacement for cement. Res Eng Struct Mater. 2023;x(x):1-15. https://doi.org/10.17515/resm2023.48ma0725rs.
[5] Sahib Q, Marshdi R, Dakhil AJ, Al-khafaji Z. Investigation of strength and durability performance of concrete with varying crude oil waste ratios. Res Eng Struct Mater. 2024;x(x):1-17.
[6] Vairagade VS, Dhale SA. Hybrid fibre reinforced concrete-A state of the art review. 2023. https://doi.org/10.1016/j.hybadv.2023.100035
[7] Prakash R, Mukilan M. Impact of various fibers on the mechanical and durability performance of fibre-reinforced concrete with SBR latex. 2024.
[8] Sharhan ZS, Rad MM. Elasto-plastic analysis of two-way reinforced concrete slabs strengthened with carbon fiber reinforced polymer laminates. 2024. https://doi.org/10.3390/computation12050093
[9] Cucuzza R, Aloisio A, Accornero F, Marinelli A, Bassoli E, Marano GC. Size-scale effects and modelling issues of fibre-reinforced concrete beams. Constr Build Mater. 2023;392:131727. https://doi.org/10.1016/j.conbuildmat.2023.131727
[10] Lin C, Kanstad T, Jacobsen S, Ji G. Bonding property between fiber and cementitious matrix: A critical review. Constr Build Mater. 2023;378:131169. https://doi.org/10.1016/j.conbuildmat.2023.131169
[11] Abdalla JA, et al. A comprehensive review on the use of natural fibers in cement/geopolymer concrete: A step towards sustainability. Case Stud Constr Mater. 2023;19:e02244. https://doi.org/10.1016/j.cscm.2023.e02244
[12] Dutt KS, Kumar KV, Kishore IS, Chowdary CM. Influence of natural fibers as an admix in normal concrete mix. Int J Eng Trends Technol. 2016;35(1):1-5. https://doi.org/10.14445/22315381/IJETT-V35P201
[13] Sen T, Reddy HNJ. Strengthening of RC beams in flexure using natural jute fibre textile reinforced composite system and its comparative study with CFRP and GFRP strengthening systems. Int J Sustain Built Environ. 2013;2(1):41-55. https://doi.org/10.1016/j.ijsbe.2013.11.001
[14] Elbehiry A, Elnawawy O, Kassem M, Zaher A, Mostafa M. FEM evaluation of reinforced concrete beams by hybrid and banana fiber bars (BFB). Case Stud Constr Mater. 2021;14:e00479. https://doi.org/10.1016/j.cscm.2020.e00479
[15] Suresh S, Charan MS, Kishore IS. Strength and behaviour of concrete by using natural and artificial fibre combinations. Int J Civ Eng Technol. 2017;8(4):1652-8.
[16] Kangu AN, Shitote SM, Onchiri RO, Matallah M. Effects of waste tyre steel fibres on the ultimate capacity of headed studs in normal concrete. Case Stud Constr Mater. 2023;18:e02166. https://doi.org/10.1016/j.cscm.2023.e02166

[17] Sharma U, Sheikh IM. Investigating self-compacting concrete reinforced with steel & coir fiber. Mater Today Proc. 2021;45(x):4948-53. https://doi.org/10.1016/j.matpr.2021.01.386
[18] Rajkohila A, Chandar SP, Ravichandran PT. Assessing the effect of natural fiber on mechanical properties and microstructural characteristics of high strength concrete. Ain Shams Eng J. 2024;102666. https://doi.org/10.1016/j.asej.2024.102666
[19] Nduka DO, Olawuyi BJ, Ajao AM, Okoye VC, Okigbo OM. Mechanical and durability property dimensions of sustainable bamboo leaf ash in high-performance concrete. Clean Eng Technol. 2022;11:100583. https://doi.org/10.1016/j.clet.2022.100583
[20] Saidi T, Hasan M, Amalia Z, Salsabila S. The analysis of the bond strength between natural fiber reinforced polymer (NFRP) sheets and concrete. Results Eng. 2023;18:101124. https://doi.org/10.1016/j.rineng.2023.101124
[21] Yinh S, et al. Strengthening effect of natural fiber reinforced polymer composites (NFRP) on concrete. Case Stud Constr Mater. 2021;15:June. https://doi.org/10.1016/j.cscm.2021.e00653
[22] Al Ghali AE, El Ezz NE, Hamad B, Assaad J, Yehya A. Comparative study on shear strength and life cycle assessment of reinforced concrete beams containing different types of fibers. Case Stud Constr Mater. 2023;19:e02497. https://doi.org/10.1016/j.cscm.2023.e02497
[23] Althoey F, Zaid O, Majdi A, Alsharari F, Alsulamy S, Arbili MM. Effect of fly ash and waste glass powder as a fractional substitute on the performance of natural fibers reinforced concrete. Ain Shams Eng J. 2023;14(12):102247. https://doi.org/10.1016/j.asej.2023.102247
[24] Ahdal AQ, et al. Mechanical performance and feasibility analysis of green concrete prepared with local natural zeolite and waste PET plastic fibers as cement replacements. Case Stud Constr Mater. 2022;17:e01256. https://doi.org/10.1016/j.cscm.2022.e01256
[25] Mohammed AA, Muhammad MA, Mohammed BK. Effect of PET waste fiber addition on flexural behavior of concrete beams reinforced with GFRP bars. Case Stud Constr Mater. 2023;19:e02564. https://doi.org/10.1016/j.cscm.2023.e02564
[26] Abdulateef LA, Hassan SH, Ahmed AM. Exploring the mechanical behavior of concrete enhanced with fibers derived from recycled plastic bottles. Eng Technol Appl Sci Res. 2024;14(2):13481-6. https://doi.org/10.48084/etasr.6895
[27] Sharma L, Viradiya J, Gupta R, Baker S. Converting other flexible plastic packaging into fiber reinforcement for concrete structures. Lect Notes Civ Eng. 2024;359:885-901. https://doi.org/10.1007/978-3-031-34027-7_59
[28] Yıldızel SA, et al. Experimental investigation and analytical prediction of flexural behaviour of reinforced concrete beams with steel fibres extracted from waste tyres. Case Stud Constr Mater. 2023;19:June. https://doi.org/10.1016/j.cscm.2023.e02227
[29] Kishore IS, Chowdary CM. Influence of steel fibers as admix in normal concrete mix. Int J Civ Eng Technol. 2016;7(1):93-103.
[30] Pham LT, Trinh TD, Do QT, Huang JY. Flexural behavior of printed concrete wide beams with dispersed fibers reinforced. Res Eng Struct Mater. 2023;x(x):1-16.
[31] Zhang Y, Xin H, Correia JAFO. Fracture evaluation of ultra-high-performance fiber reinforced concrete (UHPFRC). Eng Fail Anal. 2021;120:September.
[32] Al-Jasmi S, Ariffin NF, Abu Seman M. Model analysis of carbon fiber reinforcement properties for reinforced concrete beams to resist blast loads. Mater Today Proc. 2023;xxxx. https://doi.org/10.1016/j.matpr.2023.06.326
[33] Kishore IS, Chowdary CM, Rao VR. Effect of debonding on stiffness and long-term creep of sandwich panels. IOP Conf Ser Mater Sci Eng. 2020;993(1). https://doi.org/10.1088/1757-899X/993/1/012169

[34] Yoo DY, et al. Strain-hardening effect on the flexural behavior of ultra-high-performance fiber-reinforced concrete beams with steel rebars. Dev Built Environ. 2024;17:100343. https://doi.org/10.1016/j.dibe.2024.100343
[35] Qasim M, Lee CK, Zhang YX. Flexural strengthening of reinforced concrete beams using hybrid fibre reinforced engineered cementitious composite. Eng Struct. 2023;284:115992. https://doi.org/10.1016/j.engstruct.2023.115992
[36] Amaireh LK, Al-Tamimi A. Optimum configuration of CFRP composites for strengthening of reinforced concrete beams considering the contact constraint. Procedia Manuf. 2020;44:350-7. https://doi.org/10.1016/j.promfg.2020.02.284
[37] Sajedi SF, Saffarian I, Pourbaba M, Yeon JH. Structural behavior of circular concrete columns reinforced with longitudinal GFRP rebars under axial load. Buildings. 2024;14(4):988. https://doi.org/10.3390/buildings14040988
[38] Li C, Li Q, Li X, Zhang X, Zhao S. Elasto-plastic bending behaviors of steel fiber reinforced expanded-shale lightweight concrete beams analyzed by nonlinear finite-element method. Case Stud Constr Mater. 2020;13(36). https://doi.org/10.1016/j.cscm.2020.e00372
[39] Farooq MA, Fahad M, Ali B, Ullah S, El Ouni MH, Elhag AB. Influence of nylon fibers recycled from the scrap brushes on the properties of concrete: Valorization of plastic waste in concrete. Case Stud Constr Mater. 2022;16:e01089. https://doi.org/10.1016/j.cscm.2022.e01089